Photodisintegration of 1p-shell nuclei

N. G. Goncharova

Moscow State University

H. -R. Kissener

Central Institute of Nuclear Research, Rossendorf, GDR

R. A. Éramzhyan

Institute of Nuclear Research, USSR Academy of Sciences, Moscow

Fiz. Elem. Chastits At. Yadra **16**, 773–823 (July–August 1985)

The main characteristics of the giant dipole resonance in 1p-shell nuclei—the energy dependence of the cross section of total photodisintegration together with the partial (γ, n_i) and (γ, p_i) cross sections—are considered. Possibilities of describing these characteristics in microscopic approaches based on the many-particle shell model are discussed.

INTRODUCTION

The giant photonuclear resonance is a phenomenon observed in all nuclei—from the lightest to the heaviest. In medium and heavy nuclei, if they are spherical, a single maximum is formed in the giant resonance, and the nuclear shell-structure effects are weakly manifested. A different situation is realized in light nuclei, particularly in 1p-shell nuclei. In this case, a single peak is not formed, and the resonance consists of several broad maxima and extends to very high excitation energies of the nucleus. In the 1p-shell nuclei, the nucleon–nucleon interaction is incapable of suppressing the shell-structure effects and cannot form a single peak. This aspect of the photonuclear resonance in 1p-shell nuclei was already noted in the earliest stage in the investigations[1–5] on the basis of a simple approach to the description of the resonance as a superposition of doorway particle–hole configurations.

To describe the resonance more realistically, it was necessary to make extensive calculations, taking into account the coupling of the doorway states to more complicated states. Further, since the 1p-shell nuclei have well-defined individual properties, it was necessary to make systematic calculations for each of them. A further important stimulus for detailed investigation of the photonuclear resonance in 1p-shell nuclei is the possibility of experimental separation of the partial photodisintegration cross sections, i.e., the cross sections with a fixed final state of the resulting nuclear system.[6,7] The investigations of the partial cross sections revealed the fractional-parentage coupling of the giant resonance to the low-lying states of the final nucleus, the structure of these states being established rather well. Through the partial spectra one can test theory much more thoroughly and establish the extent to which it can describe the giant resonance. On the theory side, such a program has been realized for many years, primarily at the Joint Institute for Nuclear Research (Dubna), the Central Institute of Nuclear Research (Rossendorf, GDR), and the Scientific-Research Institute of Nuclear Physics at Moscow State University. The present review is based on the results of these investigations; it summarizes the results of the theoretical study of the general and specific features of the excitation and decay of the photonuclear resonance in 1p-shell nuclei. We shall not dwell in detail on the specific problems associated with the phenomenon of configuration splitting of the dipole resonance; this has been discussed in detail in the review of Ref. 6.

The partial spectra of the photodisintegration of 1p-shell nuclei have been discussed in a number of reviews.[8–11] The information available at the time of their writing was rather disconnected, so that a unified picture covering the complete range of nuclei from $A = 6$ to $A = 16$ could not be established. Subsequent measurements of the partial spectra have made possible a more systematic comparison of theory and experiment.

The review begins with a discussion of the microscopic approach to the description of dipole excitation of a nucleus and its subsequent decay. The following section is devoted to a discussion of the energy dependence of the cross sections of total absorption and the integrated characteristics of the dipole resonance. Then follows a discussion of the main features in the decay of the photonuclear resonance. The study of specific nuclei begins with ^{12}C. This nucleus is one of the most popular objects of microscopic nuclear theory. Comparison of the results with the extensive experimental data makes it possible to establish the limits of applicability of the theoretical approaches and to understand the physical reasons for the discrepancy between theory and experiment. Other nuclei in the middle and at the end of the 1p shell with zero isospin of the ground state are discussed in the same section.

The following section is devoted to nuclei in the middle and at the end of the 1p shell for which the ground-state isospin is nonzero. Study of their photodisintegration makes possible an advance in understanding questions such as the isospin splitting of the resonance. A separate section is devoted to the nuclei at the beginning of the 1p shell.

1. FUNDAMENTALS OF THE PHOTODISINTEGRATION THEORY FOR LIGHT NUCLEI

Methods of describing photodisintegration of light nuclei

Essentially two approaches are used to describe the photodisintegration of light nuclei. One, the continuum

 0090-4759/85/040337-27$04.40

shell model (CSM), is based on the unified theory of nuclear reactions and takes into account directly the fact that the giant resonance is in the region of the continuum. The other is the traditional bound shell model (BSM) approach, which is based on a model that does not take into account the coupling of the quasistationary states to the continuum.

Several forms of the unified theory are known.[12-15] They differ mainly in the assumptions used to simplify the numerical calculations. One of them is based on the method of strong channel coupling and Feshbach's projection-operator formalism. It is described in detail in the review of Ref. 14. In this form of the theory, the basis of functions employed is divided into two subspaces, one of which, Q, contains all the states of the discrete spectrum and the single-particle resonances and is identical to the basis of the traditional shell model without allowance for the continuum. The remainder of the wave function, including the scattering states, belongs to the P subspace.

Following Ref. 14, we write the expression for the matrix element of the transition of the nuclear system from the ground state $|0\rangle$ to the state $\psi_f(E)$ under the influence of the perturbation H_{int} in the form

$$M_{f0}(E) = \langle \Psi_f^- (E) | H_{\text{int}} | 0 \rangle = \langle \varphi_f^- (E) | H_{\text{int}} | 0 \rangle + \sqrt{1/2\pi} \sum_\rho \frac{\gamma_{f\rho} W_{\rho i}}{E - E_\rho + i\Gamma_\rho(E)/2}. \quad (1)$$

The first term takes into account direct transition to the P subspace. It depends smoothly on the energy. The second term is the amplitude of a two-step resonance transition, and it can be represented in the form of the diagram

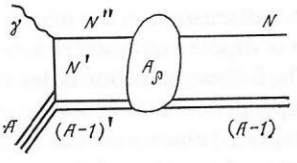

The contribution of each resonance ρ to the channel f is determined by the transition matrix element $W_{\rho i}$ and the decay amplitude $\gamma_{f\rho}$:

$$\gamma_{f\rho} = \sqrt{2\pi} \langle \varphi_f^- (E) | H | \Phi_\rho^+ \rangle. \quad (2)$$

In the neighborhood of an isolated resonance, the contribution of the first term can be ignored in (1), and in the sum we can restrict ourselves to a single term, which determines the transition probability associated with the resonance ρ:

$$\Lambda_\rho = \frac{1}{2\pi} \int dE \frac{\sum_f |\gamma_{f\rho}|^2}{(E - E_\rho)^2 + (\Gamma_\rho/2)^2} |W_{\rho i}|^2. \quad (3)$$

Usually, the weak dependence of Γ_ρ and E_ρ on the energy E is ignored. Then for the isolated resonance

$$\sum_f |\gamma_{f\rho}|^2 = \Gamma_\rho, \quad (4)$$

and the expression for the transition probability becomes

$$\Lambda_\rho \doteq |\langle \Phi_\rho^- | H_{\text{int}} | 0 \rangle + \langle Q\Phi_\rho^- | H_{\text{int}} | 0 \rangle|^2. \quad (5)$$

Here, Φ_ρ^- is the resonance wave function, an eigenfunction of the Hamiltonian

$$H_{QQ}^{\text{eff}} = QHQ + QHP\,[E - PHP]^{-1} PHQ. \quad (6)$$

The second term in (6) is the result of the coupling of the continuum to the discrete states. In (2) and (6), H is the Hamiltonian of the interaction of the nucleons in the nucleus.

If the coupling of the discrete states to the continuum is ignored in (5), then for the probability of a transition with excitation of an isolated resonance we obtain

$$\tilde{\Lambda}_\rho = |\langle \Phi_\rho^- | H_{\text{int}} | 0 \rangle|^2. \quad (7)$$

The traditional shell model without allowance for the continuum (BSM) is realized when the calculation of Φ_ρ^- in (7) is based, not on the Hamiltonian (6), but on one in which its second term is ignored, i.e.,

$$H_{\text{BSM}} = QHQ. \quad (8)$$

The description of the decay characteristics of a resonance in the BSM approach is based on R-matrix theory and the reduced-width formalism.[16] The partial width of resonance ρ with respect to emission of a nucleon (or nucleon association) with quantum numbers λ (n, l, j) and formation of the daughter nucleus in the state β $(E_\beta; J_\beta, T_\beta)$ is described by

$$\Gamma_{\beta\lambda} = 2k\gamma_0^2 P_{\beta\lambda}(E_\beta) S_{\beta\lambda}. \quad (9)$$

In (9), k is the wave number of the relative motion of the emitted particle and the residual nucleus, $P_{\beta\lambda}(E_\beta)$ is the factor that determines the barrier penetrability, $S_{\beta\lambda}$ is a spectroscopic factor:

$$S_{\beta\lambda} = N \langle \rho \| \beta, \lambda \rangle^2, \quad (10)$$

γ_0^2 is the reduced single-particle width,

$$\gamma_0^2 = \frac{\hbar^2}{\mu_c a_c} \frac{1}{2} a_c^3 R_0^2(a_c), \quad (11)$$

μ_c is the reduced mass of the decay products, a_c is the channel radius, and $R_c(a_c)$ is the value of the radial wave function of the nucleon on the surface of the channel. It is customary to use a value of γ_0^2 constant for all channels and equal to $\hbar^2/\mu_c a_c$.

In the framework of the traditional shell model, the integrated cross section for photodisintegration of the nucleus through the isolated resonance ρ with formation of the daughter nucleus in the state β is written in the form

$$\sigma_{\rho\beta} = \sigma_\rho \Gamma_{\rho\beta} / \sum_\mu \Gamma_{\rho\mu}, \quad (12)$$

where $\Gamma_\rho = \Sigma_\mu \Gamma_{\rho\mu}$ is the total width of the resonance.

Calculations in the framework of the unified theory are technically complicated even when a small number of channels of the simplest configuration are taken into account. The main difficulty of the approach is the limited number of configurations that can be included in the calculation. It is therefore nuclei with closed shells or their neighbors (^{12}C, ^{13}C, ^{16}O) that have been investigated in such an approach. The calculations have made it possible to establish the regions of applicability of the models that do not take into account directly the coupling of the quasistationary states to the continuum. The importance of calculations in the CSM was above all that they provided a basis for the calculations in the BSM approach. In contrast to the unified theory, it is not difficult in the traditional shell model to take into account the mixing of a large number of configurations,

TABLE I. Structure of ground-state wave functions of 1p-shell nuclei[18,20] [Hamiltonian variant (8–16)2BME].

Nucleus	J	T	Configuration $(n_1, n_2) \equiv P_{3/2}^{n_1} P_{1/2}^{n_2}$					Weight, %				
			1	2	3	4	5	1	2	3	4	5
^{7}Li	3/2	1/2	(3,0)	(2,1)	(1,2)	—	—	58	16	26	—	—
^{9}Be	3/2	1/2	(5,0)	(4,1)	(3,2)	(1,4)	—	51	17	28	3	—
^{10}B	3	0	(6,0)	(5,1)	(4,2)	(3,3)	(2,4)	58	19	20	2	1
^{11}B	3/2	1/2	(7,0)	(6,1)	(5,2)	(4,3)	(3,4)	48	7	38	5	3
^{12}C	0	0	(8,0)	(6,2)	(5,3)	(4,4)	—	40	43	7	10	—
^{13}C	1/2	1/2	(8,1)	(6,3)	(5,4)	—	—	73	26	1	—	—
^{14}N	1	0	(8,2)	(7,3)	—	—	—	90	10	—	—	—
^{14}C	0	1	(8,2)	(6,4)	—	—	—	85	15	—	—	—
^{15}N	1/2	1/2	(8,3)	—	—	—	—	100	—	—	—	—

something which is necessary in order to describe the observed spread of the doorway states. It is therefore natural that the most detailed information on the disintegration of light nuclei has been obtained in the framework of the traditional approach.

The problem of describing the reduced nucleon widths in the BSM has been the subject of much discussion. The partial widths of the resonances in the two approaches (CSM and BSM)—the expressions (4) and (9)—were compared in detail in Ref. 15. It was concluded that, despite the differences in their absolute values, their relative values in the CSM and BSM are fairly close to each other if the decay proceeds to hole states. It should be noted that in calculations of the photodisintegration of 1p-shell nuclei in the framework of the CSM one also introduces an optical potential[17] in order to reduce the cross section in the region of the giant resonance and give the quasistationary states a finite width.

Configuration space of the dipole-resonance states in 1p-shell nuclei

The description of 1p-shell nuclei is usually based on the assumption that the ground and low-lying states are described by the configuration $1s^4\,1p^{A-4}$, where A is the number of nucleons of the nucleus. The wave function $\Psi(JT)$ of such states is the superposition

$$\Psi(JT) = \sum_{LS,\,\lambda} \alpha(LS,\ [\lambda])\,|1p^{A-4}\,[\lambda]\ T(LS)\,J\rangle, \qquad (13)$$

if the basis is chosen in the LS representation, and

$$\Psi(JT) = \sum_{J_1T,\ J_2T_2n_1n_2} \alpha(J_1T_1,\ J_2T_2,\ n_1n_2)\,|1p_{3/2}^{n_1}J_1T_1,\ 1p_{1/2}^{n_2}J_2T_2{:}JT\rangle, \qquad (14)$$

if the basis is chosen in the jj representation; $[\lambda]$ is a Young diagram. The numerical values of the coefficients α are found by diagonalizing the energy matrix.[18,19] The distribution of the nucleons over the subshells is given in Table I for the ground states of the nuclei. The weights of the dominant components in the LS representation[19] are given in Table II. The admixture of higher configurations corresponding to transition of a nucleon to higher shells is, as a rule, ignored. We note that in the ground state of ^{16}O this admixture is about 20%.

In the construction of the dipole-resonance states, a restriction is usually made to transitions of a nucleon within a band, corresponding to $1\hbar\omega$ excitations. Then three types of configuration,

$$\left.\begin{aligned} &1s^4 1p^{A-5}2s;\\ &1s^4 1p^{A-5}1d;\\ &1s^3 1p^{A-3} \end{aligned}\right\} \qquad (15)$$

form the states of the dipole resonance. There being different ways of coupling the nucleon spins, these configurations lead to a large basis. The total number of states is given in Table III.[20] States corresponding to center-of-mass motion of the nucleus are also included in the space of the basis

TABLE II. Weights of dominant components in the ground-state wave function of 1p-shell nuclei in the LS representation[19] (variant of the Hamiltonian with Rosenfeld forces).

Nucleus	Main component $[\lambda]^{2T+1}\,^{2S+1}L_J$	Weight,%	Nucleus	Main component $[\lambda]^{2T+1}\,^{2S+1}L_J$	Weight,%
^{7}Li	$[3]^{22}P_{3/2}$	97	^{12}C	$[44]^{11}S_0$	71
^{8}Be	$[4]^{11}S_0$	97	^{13}C	$[441]^{22}P_{1/2}$	64
^{9}Be	$[41]^{22}P_{3/2}$	81	^{14}N	$[442]^{13}D_1$	90
^{10}B	$[42]^{13}D_3$	64	^{14}C	$[442]^{31}S_0$ $[433]^{33}P_0$	56 44
^{11}B	$[43]^{22}P_{3/2}$ $[43]^{22}D_{3/2}$	41 32	^{15}N	$[443]^{22}P_{1/2}$	100

TABLE III. Dimension in the complete basis of $1\hbar\omega$ excitations of the configuration space of dipole excitations of $1p$-shell nuclei.[20] The number of spurious states is indicated in the brackets.

Nucleus	T_f	1/2			3/2		
	J_i \ J_f	1/2+	3/2+	5/2+	1/2+	3/2+	5/2+
^{7}Li	3/2−	36(10)	52(14)	45(11)	21(4)	29(5)	24(4)
^{9}Be	3/2−	97(21)	148(32)	146(31)	66(12)	99(17)	91(14)
^{11}B	3/2−	125(21)	197(32)	199(31)	89(12)	136(17)	131(14)
^{13}C	1/2−	75(10)	115(14)	—	48(4)	72(5)	—
^{15}N	1/2−	18(2)	25(2)	—	8(0)	11(0)	—

Nucleus	T_f	1				
	J_i \ J_f	0−	1−	2−	3−	4−
^{10}B	3+	—	—	190(30)	157(25)	96(11)
^{12}C	0+	—	141(17)	—	—	—
^{14}N	1+	20(1)	50(5)	56(3)	—	—
^{16}O	0+	—	5(0)	—	—	—

Nucleus	T_f	1	2
	J_i \ J_f	1−	1−
^{14}C	0+	50(5)	13(0)

configurations. These configurations can be completely separated, and the subsequent calculation of the dipole excitations is made in the basis corresponding solely to excitation of the internal degrees of freedom of the nucleus. The maximal number of basis states in the band of the $1\hbar\omega$ excitations after separation of the states corresponding to the center-of-mass motion is 168 for the levels with the quantum numbers $J^{\pi}T = 5/2^{+}\ 1/2$ in 11_{B}. Technical difficulties arise in practical work with such a large basis. Therefore, not all $1p$-shell nuclei are included in the complete basis. Calculations have been made for the nuclei ^{6}Li (Refs. 6, 11, and 20–23), ^{7}Li (Refs. 20, 24, and 25), ^{9}Be($T = 3/2$) (Refs. 20 and 25), 11_{B} (Refs. 20 and 26), ^{12}C (Refs. 20, 27, and 28), ^{13}C (Refs. 20, 29, and 30), ^{14}N (Refs. 20, 22, 23, and 30–32), ^{14}C (Refs. 20, 31, and 32), ^{15}N (Refs. 11, 20, 33, and 34). Instead of the basis (15), one can use the equivalent basis

$$\begin{aligned} &|\,1s^{4}1p^{A-5}(J'T'E');\ 2s:JT\rangle;\\ &|\,1s^{4}1p^{A-5}(J'T'E);\ 1d:JT\rangle;\\ &|\,1s^{3}1p^{A-4}(J'T'E');\ 1p:\ JT\rangle. \end{aligned} \tag{16}$$

Here, $|J'T'E'\rangle$ is the wave function of the state of the nucleus with A–1 nucleons, total angular momentum J', isospin T', and energy E'.

The second approach begins to exhibit its advantages when the basis is truncated in order to simplify the calculations. One of the ways to achieve such a simplification was proposed in Ref. 35: In the basis, one includes only those states of the A–1 nucleus that have a fractional-parentage coupling to the ground state (J_0T_0) of the A nucleus, i.e., states for which the expansion coefficient $\langle A, J_0T_0\|A-1, J'T'E';j\rangle$ is not small:

$$\begin{aligned} \Psi(J_0T_0) = \sum_{J'T'E',\,j} &< A,\ J_0T_0\,\|\,A-1,\\ &J'T'E';\ j>|\,A-1,\ J'T'E'\ ;1p_j\rangle. \end{aligned} \tag{17}$$

The states $|A-1, J'T'E'\rangle$ of the A–1 nucleus are usually called $1p_j$ hole states of the original nucleus A. In the nuclei from ^{12}C to ^{16}O, transitions from the $1s$ shell can be ignored. The number of configurations involved in the calculations in such an approach depends on the structure of the ground state. For example, the fractional-parentage structure of the ground state of ^{11}B is exhausted to 97%, provided the calculation includes 15 states of the nucleus with $A = 10$. We shall refer to this as the "particle over the final-nucleus states" (PFNS) approach. The number of basis functions in such a truncation procedure is much smaller than in the complete calculation that takes into account all the functions in the $1\hbar\omega$-excitation band. The approach allows extension of the basis by the inclusion in it of levels of the A–1 nucleus having a fractional-parentage coupling to the lowest collective states of the nucleus A. In the PFNS approach there are also two versions.

In one, a continuum wave function is used to describe the motion of the particle; in the other, the function of an infinitely deep well. In the PFNS approach, the dipole resonance has been calculated in the following nuclei: ^{12}C (Refs. 35–37), ^{13}C (Ref. 38), ^{14}N (Ref. 39), ^{15}N (Ref. 39), ^{11}B (Ref. 40), and ^{10}B (Ref. 41).

Unfortunately, there has been no systematic comparison of the two approaches for an optimal description of the giant-resonance structure. A basis reduction was made in Ref. 28 for ^{12}C. First, the complete basis of excitations was used, and then only six low-lying states of the $A = 11$ nucleus of negative parity were retained. Spurious states were eliminated. Then the case when they are not eliminated was considered. The conclusion reached was that allowance for the complete basis leads to the formation of additional structure in the spectrum of the dipole excitations compared with the case of the truncated basis. However, the gross structure

of the spectrum is not changed. If the spurious states are not separated, the maximum of the cross section is shifted to lower energies. We note that in a calculation with a complete basis the position of the main peak is lower than the experimental position. However, the procedure of matching it to the experimental data can lead to a rearrangement of the wave functions and a change in the structure of the total-absorption curve.

Choice of the residual nucleon-nucleon interaction

To describe the interaction between the nucleons in the nucleus one uses various sets of phenomenological potentials containing central, spin-orbit, and sometimes tensor components:

$$\left.\begin{aligned} V(r) &= V^C(r) + V^{LC}(r) + V^T(r);\\ V^C(r) &= V_0^C f^C(r)\{a_{00}^C P^{00} + a_{10}^C P^{10} + a_{01}^C P^{01} + a_{11}^C P^{11}\};\\ V^{LS}(r) &= V_0^{LS} f^{LS}(r)\,(\mathrm{LS})\{a_{01}^{LS} P^{01} + a_{11}^{LS} P^{11}\};\\ V^T(r) &= V_0^T f^T(r)\, S_{12}(a_{01}^T P^{01} + a_{11}^T P^{11}). \end{aligned}\right\} \quad (18)$$

Here, $f(r)$ is the radial part of the potential, generally chosen in Gaussian or Yukawa form; P^{TS} are projection operators. The parameters a_{TS} of the potential are chosen to reproduce either the position of the low-lying levels of corresponding parity or the position of the maximum of the dipole resonance. The interaction of the $1p$-shell nucleons is usually described by the set of interaction parameters proposed in Ref. 18—the variant (8–16) 2BME. The interaction parameters for nucleons in different shells were chosen for the case of purely central forces from Ref. 42 (these are henceforth referred to as COP or Ref. 43 (called henceforth CAL). There is a further variant of the interaction,[44,45] which also includes a contribution of noncentral forces; this will be referred to as MK. The parameters of the potentials used in studies of the dipole excitations of the $1p$-shell nuclei are given in Table IV. In studies based on the PFNS approach a central potential with mixing parameters a_{TS} in the variants of Rosenfeld and Gillet[42] has been used (Table IV). The influence of the mixing parameters on the photoexcitation function is not so critical—the listed parameter sets give a satisfactory description of the localization and gross structure of the resonance. However, the situation with regard to the partial cross sections is different—in a number of cases, variation of the mixing parameters radically changes the energy distribution of the cross sections and the relationship of the channels (see Sec. 4).

TABLE IV. Parameters of nucleon–nucleon interactions.

A. Central interactions

$$f(r) = e^{-r^2/\mu^2} - (G);\quad f(r) = \frac{1}{r} e^{-r/\mu} - (Y)$$

Variant	a_{00}^C	a_{01}^C	a_{10}^C	a_{11}^C	$f(r)$	b/μ *	$-V_0$, MeV
Gillet-1	0,60	1,00	0,60	−0,60	G	1,03	45
Gillet (COP)	0,59	1,00	0,59	−0,57	G	1,01	41,6
Gillet (CAL)	−0,65	1,00	0,50	−0,15	G		55
Gillet-2	0,50	1,00	0,40	−0,50	G	1—1,2	40—45
Rosenfeld	−1,78	1,00	0,60	−0,34	G	1,03	45
					Y	μ=1,5 фм	50
MK	−0,714	1,00	0,60	−0,286	Y	1,18	44,8

B. Noncentral part (MK)

Forces	a_{01}	a_{11}	$f(r)$	b/μ *	$-V_0$, MeV
LS	1,00	3,5	Y	2.36	26
T	1,00	−0,38	Y	1.18	16,25

*b is the parameter of the oscillator functions.

2. MAIN FEATURES OF THE EXCITATION OF THE DIPOLE RESONANCE IN 1p-SHELL NUCLEI

Energy dependence of the total-absorption cross section

One of the main characteristics of photonuclear reactions is the energy dependence of the cross section for total absorption of photons: $\sigma(E_\gamma)$. This characteristic has been measured directly in $1p$-shell nuclei in Li, Be, C, O (Ref. 46), and N (Ref. 47) (Fig. 1). In Li and Be, in which the filling of the $1p$ shell is only just beginning, the photonuclear resonance is strongly smeared, and $\sigma(E_\gamma = 40\ \mathrm{MeV})$ is only half of its maximal value, reached at $E_\gamma \approx 20$ MeV. However, already for ^{12}C a fairly clear maximum is formed, though the region of localization of the resonance is still large. The situation is quite different from the one in medium and heavy nuclei, in which we observe a single (in spherical nuclei) very clear peak, the complete resonance is localized in a small energy interval, and the change in the structure of the resonance on the transition from nucleus to nucleus is small.

Overall, the theory reproduces the experimentally observed energy dependence of the total-absorption cross section in the $1p$-shell nuclei. This cross section has been calculated for $1p$-shell nuclei in a huge number of papers. In most of them, the treatment was restricted to one or two nuclei. Only in one series of studies, in Refs. 20, 24, 25, and 29–32, was use made of a unified set of parameters to calculate the

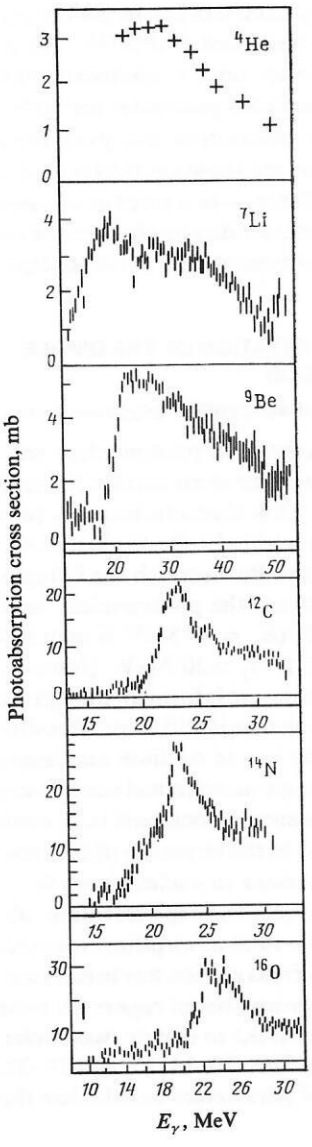

FIG. 1. Results of measurements of total photoabsorption cross sections in the nuclei Li, Be, ^{12}C, ^{16}O (Ref. 46), ^{14}N (Ref. 47), and ^{4}He (Ref. 48).

photoabsorption and photodisintegration cross sections for a large number of $1p$-shell nuclei. Figure 2 shows the results of this analysis.[20] It was made on a complete basis of configurations with the COP set (Table IV) of parameters of the residual interaction between the nucleons.

The curves were obtained by summing the contributions of all (including weak) transitions under the assumption that the resonances have a Breit-Wigner shape. The width of each was taken to be $\Gamma = 2$ MeV. The broken curve represents the branch of the resonance with isospin $T_f = T_< = T_0$, where T_0 is the isospin of the ground state of the target nucleus. The continuous curve represents the total contribution of the two isospin branches $T_<$ and $T_> = T_0 + 1$. For the nuclei ^{9}Be and ^{11}B, only the $T_> = 3/2$ branch was included in the complete basis.

The positions of the maxima of the dipole resonance are reproduced overall with accuracy 1–2 MeV in all cases except for the lightest nuclei. In the lightest nuclei (^{7}Li, ^{9}Be) the calculations gave a number of maxima absent experimentally. Such discrepancies were particularly pronounced in the region of the $1s \rightarrow 1p$ transitions ($E_\gamma > 25$ MeV). If one uses the widths obtained in the framework of R-matrix theory (as a rule, they appreciably exceed 2 MeV), the sharp peaks disappear and the agreement with experiment is improved.

The strong dependence of the cross section $\sigma(E_\gamma)$ as a function of the energy on the number of nucleons in the nucleus is associated in accordance with the theory with the following factors.

1. In the nuclei at the beginning of the $1p$ shell (^{6,7}Li and ^{9}Be) the resonance is formed mainly by transition of a nucleon from the deep $1s$ shell, this leading to excitation of the high-energy region ($E_\gamma > 25$ MeV). At the same excitation energies, the dipole resonance in ^{4}He is localized.[48] Transitions from the valence $1p$ shell in nuclei with $A = 6$–9 form the low-energy branch of the resonance ($E_\gamma \leqslant 20$–25 MeV). This specific feature of the dipole resonance in light nuclei has become known as *configurational splitting*.[1,4,5] For a detailed discussion of this phenomenon, see the reviews of Ref. 6.

2. As the $1p_{3/2}$ subshell is filled, it plays a more important part in the formation of the resonance. At the same time, the effect of the Pauli principle is manifested more and more clearly, the number of possible states that can be associated with a $1s$-$1p_{3/2}$ transition being reduced. Therefore, already in ^{9}Be the contributions of the transitions from the $1s$ and $1p$ shells become comparable, and in nuclei with $A \gtrsim 10$ the closed $1s$ shell is hardly manifested in the photonuclear resonance. In Fig. 2, the transitions that lie to the right of the line intersecting the figure obliquely are due predominantly to nucleons of the $1s$ shell. Already in the nuclei in the middle and at the end of the $1p$ shell the main maximum of the dipole photoabsorption is associated with the configuration $1p_{3/2}^{n_1-1}1p_{1/2}^{n_2}1d_{5/2}$ (see Table I).

3. As soon as "fouring" of nucleons, i.e., the appearance of four nucleons with orbital symmetry $[\lambda] = [4]$ (see Table II), occurs in the $1p$ shell, the fraction of dipole transitions associated with the $1p$ nucleons is shifted in the direction of the maximum formed by the $1s$ nucleons. The breakup of four such nucleons requires much more energy of the photons, and this leads to the appearance of a stable maximum in the region of excitation energies 20–25 MeV. This energy shift can be clearly seen in a comparison of the excitation cross sections of the nuclei ^{7}Li and ^{9}Be.

4. In the odd nuclei of the $1p$ shell and in ^{14}C there are two branches of the dipole resonance. The branch $T_<$ makes an appreciable contribution to the region of low excitation energies of the nucleus, forming the so-called pigmy resonance. In the region beyond the main maximum, the theory also predicts an appreciable contribution of the $T_<$ branch.

Now that we have discussed the general features in the excitation of the photonuclear resonance, we turn to a detailed comparison of theory with experiment. It is helpful to begin this comparison with the even nuclei in the middle and at the end of the $1p$ shell, where the resonance has already been formed, i.e., with the nuclei ^{12}C and ^{14}N.

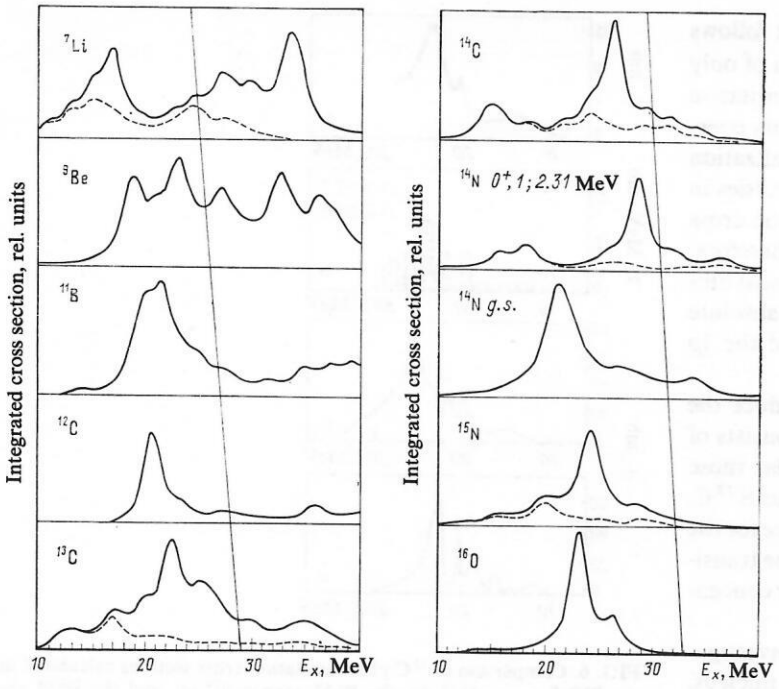

FIG. 2. Photoexcitation spectrum of $1p$-shell nuclei calculated on a complete basis of $1\hbar\omega$ excitations in the COP variant.[20] The line running obliquely through the figures separates the contributions of the $1s$ nucleons (right-hand side) from those of the $1p$ nucleons (left-hand side).

Photoabsorption cross section in even nuclei

For the example of the ^{12}C nucleus, we first illustrate the evolution of the model ideas used to describe the dipole resonance in $1p$-shell nuclei. If we assume that the $1p_{3/2}$ subshell in the ground state of ^{12}C is closed, then the resonance in this nucleus will be formed by states described by a superposition of $1p_{3/2}^{-1}$ ($2s$ or $1d$) and $1s^{-1}1p_{1/2}$ configurations. Such an approximation leads to a clear configurational splitting of the resonance: The first maximum ($E^* = 20$–22 MeV), which takes about 75% of the intensity, is associated with transitions from the $1p_{3/2}$ subshell; the second ($E^* \sim 35$ MeV), with transitions from the $1s$ shell. Figure 3a shows the result obtained in such an approximation in the CSM approach.[49] However, it does not reflect the real picture.

The results of dipole-resonance calculations with allowance for the fact that the $1p_{3/2}$ subshell is not closed, realized in the PFNS approach,[35] are given in Fig. 3b. The system of basis configurations included not only states of the $A = 11$ final nucleus having a fractional-parentage coupling to the ^{12}C ground state but also the states coupled to the first excitation ($J^\pi T = 2^+ 0$, $E^* = 4.44$ MeV). This means that the calculation includes not only the $J_n^\pi = 3/2_1^-$, $3/2_2^-$, and $1/2_1^-$ states of ^{11}B and ^{11}C but also $5/2_1^-$, $5/2_2^-$, and $7/2_1^-$. The subscript denotes the serial number of the state with given n, measured from the ground state. A similar approach was realized in the CSM method (Fig. 3c).[36] The more sophisticated model led to a more realistic picture, and a new peak appeared at $E^* \sim 26$ MeV, associated with $1p$ nucleons.

A basis of $1\hbar\omega$ excitations was taken into account more systematically for ^{14}N; all configurations in the $1\hbar\omega$-excitation band were included, and the center-of-mass motion was separated. Figure 4 shows the results of such a calculation[50]; the widths of the individual resonances were taken from calculations in R-matrix theory. The same figure gives the re-

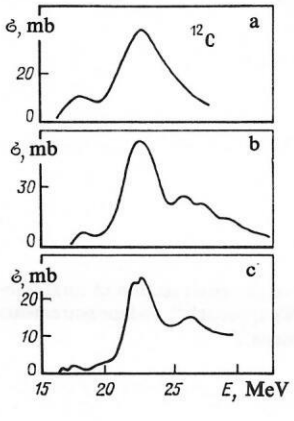

FIG. 3. Comparison of the energy dependence of the total photoabsorption cross sections in ^{12}C obtained in different theoretical approaches: a) CSM on a basis of $1p$–$1h$ configurations[49]; b) PFNS[35]; c) combined PFNS–CSM variant.[36]

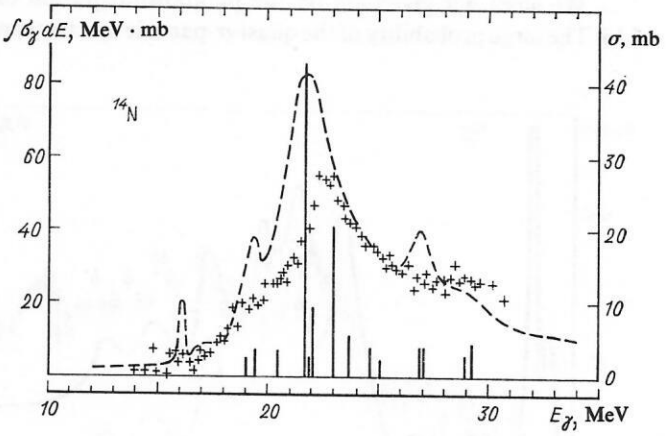

FIG. 4. Comparison of photoexcitation spectrum of ^{14}N calculated on a complete basis of $1\hbar\omega$ excitations (MK variant[50]) with the measurements of Ref. 47 (points).

sults of measurement of the total cross section.[47] It follows from the figure that the inclusion in the calculation of only the $1\hbar\omega$ configurations is inadequate to obtain quantitative agreement between theory and experiment. The theory overestimates the cross section in almost the entire localization region of the resonance. Thus, the theory has difficulties in the quantitative interpretation of the total absorption cross section but reproduces the energy dependence. Therefore, for comparison between theory and experiment we must limit ourselves to comparing the relative and not the absolute quantities. This conclusion applies to all nuclei of the $1p$ shell.

The next step, which makes it possible to reduce the concentration of the dipole transition strengths, consists of taking into account higher excitations, in particular those lying in the $2\hbar\omega$ band. This has been done for the nuclei ^{12}C, ^{16}O (see, for example, Ref. 51), and ^{15}N.[52] Allowance for the higher excitations leads to an additional spread of the transition strengths and to a significant weakening of their concentration in the region of the main maximum.

To complete the picture, we give the results of investigation of the photonuclear resonance in ^{10}B. For this nucleus, the cross sections

$$\sigma(\gamma, n_{\text{tot}}) = \sigma(\gamma, n) + \sigma(\gamma, pn) + \sigma(\gamma, 2n) + \sigma(\gamma, 2np) \quad (19)$$

have been obtained in beams of bremsstrahlung[53] and quasi-monoenergetic[54] photons. Since the contributions of the $(\gamma, 2n)$ and $(\gamma, 2np)$ channels are small,[54] it follows that (19) is almost equal to $\sigma(\gamma, 1n)$, where

$$\sigma(\gamma, 1n) = \sigma(\gamma, n) + \sigma(\gamma, pn). \quad (20)$$

The calculation of the photoabsorption cross sections in ^{10}B in the PFNS approach[41] was based on 11 states of the $A = 9$ nucleus in the energy interval from 0 to 16 MeV. The fractional-parentage structure of the ^{10}B ground state was exhausted to 99%. The calculated total photoabsorption cross section (the interaction parameters are given in row 1 of Table IV) is compared with $\sigma(\gamma, 1n)$ in Fig. 5. The theory reproduces the main feature of the observed photoabsorption spectrum—its broad localization region and the absence of sharp peaks.

We shall not give data on the photodisintegration of ^{6}Li. The large probability of the quasi-α-particle mechanism with breakup of the nucleus into several fragments makes it difficult to analyze the photodisintegration of this nucleus in the framework of the shell model. This question is considered in detail in the review of Ref. 6.

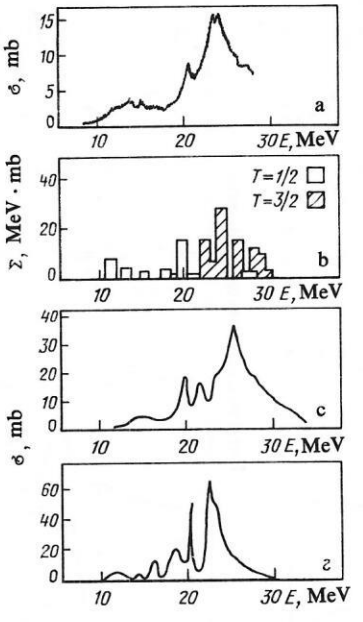

FIG. 6. Comparison of ^{13}C photoexcitation cross sections calculated in the PFNS approach[38] (b), the BSM approach[29] (c), and the BSM approach[17] (d) with the result of the measurements of Refs. 55 and 56 (a).

Photodisintegration of odd nuclei. Isospin branches of the resonance. The pygmy resonance

For the nucleus ^{13}C, the total photoabsorption cross section was obtained by adding[55,56] the measured (γ, n_{tot}) and (γ, p) cross sections. The sum is shown in Fig. 6a. We give the results of calculations of the total-absorption cross section in the PFNS approach[38] (Fig. 6b), in the COP variant of the BSM approach[29] ($1\hbar\omega$) (Fig. 6c), and in the CSM approach[17] (Fig. 6d). These variants of calculation, like many others,[15,50,57,58] differ only in the details (see Sec. 5). The attempt to identify differences between the measured cross section and any of the computational variants is not at all simple or unambiguous, since they all reflect the gross structure of the resonance.

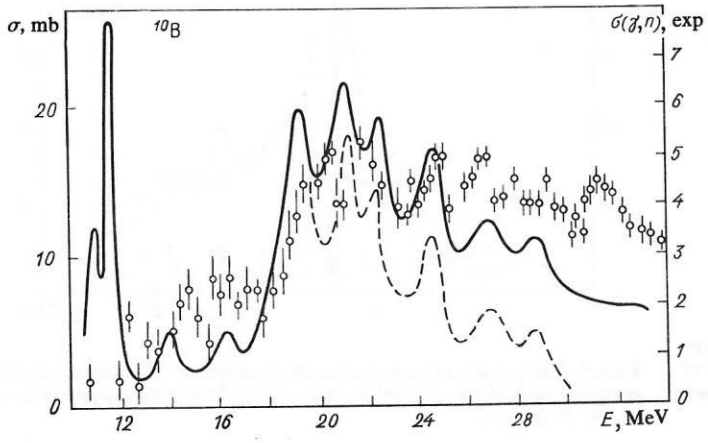

FIG. 5. Result of calculation of the cross section of total photoabsorption in ^{10}B in the PFNS approach[41] and measurements of the photoneutron cross sections.[54]

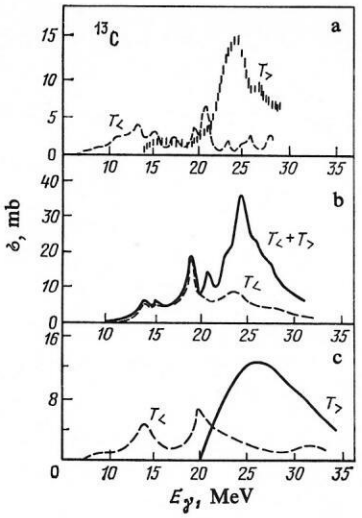

FIG. 7. Splitting of the photonuclear resonance into isospin branches in ^{13}C: a) measurement of Ref. 56; b) the result of the BSM calculation[29]; c) measurement of Ref. 59.

In Refs. 56 and 59, the cross section was decomposed into isospin branches for ^{13}C. Figure 7 shows the results together with the results of the calculation of Ref. 29. It follows from both the theory and the experiment that the low-lying region of the resonance in ^{13}C (the pygmy resonance) is formed by transitions to levels with isospin $T_<$. A certain concentration of the $T_<$ transition strengths in the region of the pygmy resonance is observed. The theory also predicts a small concentration in the region beyond the main maximum. However, overall the $T_<$ branch is more strongly distributed over the energy than the $T_>$ branch.

In ^{15}N, experimental data being absent, it is not possible to put together the total photoabsorption cross section in the manner done for the nucleus C. A restriction must therefore be made to the experimental data on the photoneutron channel (γ, n_{tot}). But this cross section also has a contribution from secondary neutrons emitted by successive decay: $^{15}\text{N}(\gamma, p)^{14}\text{C}^* \rightarrow {}^{13}\text{C} + n$. In Fig. 8, we compare the cross sections calculated in the two cases: in one, the total-absorption cross section; in the other, the sum of the $^{15}\text{N}(\gamma, n)^{14}\text{N}$ and $^{15}\text{N}(\gamma, p)^{14}\text{C}^* \rightarrow {}^{13}\text{C} + n$ cross sections. The same figure shows the measured cross section of the (γ, n_{tot}) reaction.

It follows from the calculations of Refs. 33 and 34 that in about half the cases the photonuclear resonance in ^{15}N decays into highly excited states of ^{14}N and ^{14}C, this leading to the emission of a subsequent nucleon. Secondary neutrons will be emitted mainly as a result of decay of two excited states of the nucleus ^{14}C ($J^\pi T = 2^+ 1, E^* = 10.43$ MeV and $J^\pi T = 1^+ 1$, $E^* \approx 15$ MeV). About 15% of the integrated total-absorption cross section or about 30% of the cross section in the channel $^{15}\text{N}(\gamma, n)^{14}\text{N}$ corresponds to these two levels.

The theory reproduces overall the gross structure of the resonance in this nucleus. In the region of the pygmy resonance, there is a small contribution from the $T_>$ branch. The isospin branches have not been separated experimentally in this nucleus.

A different situation in the formation of the energy regions of the resonance is realized in ^{7}Li (as in ^{6}Li). A strong transition to the region of low excitation energies is associated with $1p$ nucleons, whereas a maximum at a much higher energy is due to $1s$ nucleons. At the same time, both isospin branches are responsible for the formation in ^{7}Li of the pygmy resonance as well as the resonance itself (see Fig. 2).

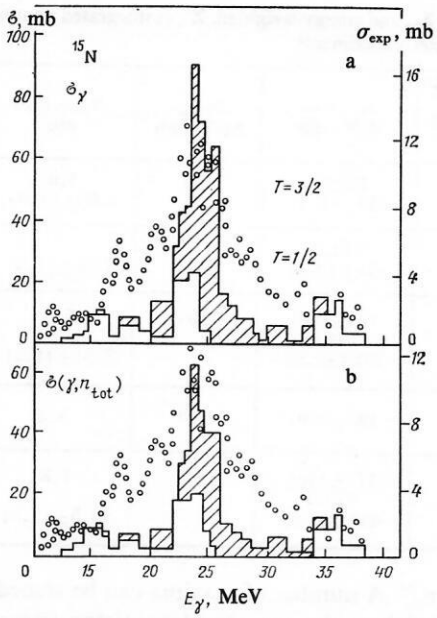

FIG. 8. Calculation of total photoabsorption cross section (a) and photoneutron cross section (b) in ^{15}N.[33,34] The experimental data on the (γ, n_{tot}) channel are taken from Ref. 60 (open circles, right-hand scale).

In ^{11}B, the theory encounters difficulties in the qualitative description of the gross structure of the total-absorption curve. In fact, this is the only $1p$-shell nucleus in which such a problem arises. Figure 9 gives experimental data on the

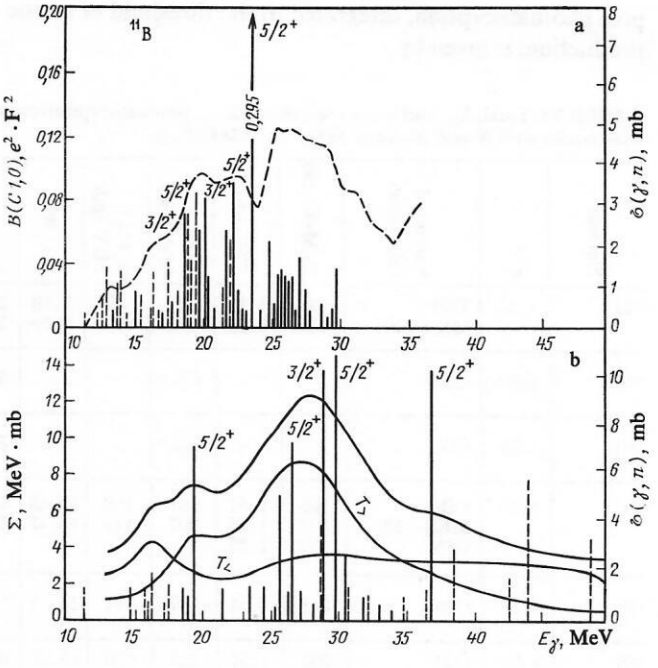

FIG. 9. Photoexcitation of the ^{11}B nucleus: a) calculation in the BSM($1\hbar\omega$) method[26] (the broken curve is the experiment of Ref. 54); b) the result of calculation in the PFNS approach.[40] The curves give the total cross sections and the cross sections of $T_<$ and $T_>$ excitations.

TABLE V. Integrated, Σ_0, and energy-weighted, Σ_{-1}, integrated photoabsorption cross sections in 1*p*-shell nuclei (experiment).

Nucleus	Interval of integration, MeV	$\Sigma_0 \pm$ (%), MeV · mb	Σ_{TRK}, MeV · mb	$\Sigma_{-1} \pm$ (%), mb	Reference
^{7}Li	52 100	123^{+30}_{-20} 143±(1.7)	103	4,9 4.64±(1.0)	[112] [46]
^{9}Be	35 100	112.2 173±(2.0)	133	5.19±(1.5)	[114] [46]
^{12}C	30 35 100	133±(10) 144.0 291±(1.6)	180	5,4 8.81±(1.1)	[47] [114] [46]
^{14}N	30	195±(19)	210	8.4	[47]
^{16}O	30 35 100	171±(10) 179.5 432±(2.0)	240	7.2 14.5±(1.3)	[47] [114] [46]

^{11}B(γ, n_{tot}) reaction.[54] A number of maxima can be traced on the background of the rather structureless photoneutron spectrum. Not less than 50% of the cross section is concentrated in the region $E_\gamma > 25$ MeV. In Fig. 9 we also give the results of a calculation in the BSM approach with a complete basis[26] and in the PFNS approach,[40] in which 15 states of the $A = 10$ nucleus were taken into account. The fractional-parentage structure of the ^{11}B ground state was exhausted to 97%. The calculation using the complete basis does not reflect the observed picture well. In the PFNS approach, after the main maximum, situated at $E = 26$ MeV, has been matched, better agreement with experiment is achieved.

Integrated photoabsorption cross sections

As follows from the sum rules, the cross section of dipole photoabsorption, integrated to the threshold of meson production, is given by

$$\sum_0 (E) = \int_0^E \sigma (E_\gamma)\, dE_\gamma = \sum_{TRK} (1 + x), \qquad (21)$$

where $\Sigma_{TRK} = 60\, NZ/A$, MeV · mb, is the value that follows from the classical Thomas-Reiche-Kuhn sum rule, while x includes the effects associated with the exchange interaction (see for example, Ref. 61).

For the 1*p*-shell nuclei, experimental data on the integrated cross sections as functions of the energy E are given in Table V. As follows from these data, in the region up to 30–40 MeV there is not always in fact exhaustion of even the part of the cross section associated with the classical sum rule. Tables VI and VII give the results of calculation of this characteristic in the BSM ($1\hbar\omega$) approach for different variants of the residual nucleon-nucleon interaction. It can be seen that there is a certain dependence on the choice of the interaction. However, the differences do not exceed 10% for

TABLE VI. Total, Σ_0, and energy-weighted, Σ_{-1}, photoabsorption cross sections in 1*p*-shell nuclei with $N \neq Z$ (theory), MK($-x$)≡MK(E_{1s}).

Nucleus	*b*, *F*	Variant of calculation	Σ_0, MeV · mb	Σ_0/Σ_{TRK}	$\Sigma_0 (T_>)$, MeV · mb	$\Sigma_0 (T_<)$, MeV · mb	Σ_{-1}, mb	$\Sigma_{-1} (T_>)$, mb	References
^{7}Li	1.45	COP MK (—20)	114 133	1.11 1.29	69 77	45 56	5.19 5.19	2.69 2.69	[20] [20]
^{9}Be	1.50	COP	—	—	104 *	—	—	3.69	[20]
^{11}B	1.55	COP	—	—	134 *	—	—	5.38	[20]
^{13}C	1.70	COP MK (—12) CSM	305 321 242	1.57 1.65 1.25	197 207 —	108 114 —	13.45 13.45 —	7.86 7.86 —	[20] [20] [15]
^{14}C	1.70	COP	318	1.54	147	171	14.27	5.55	[20]
^{15}N	1.70	COP Rosenfeld	351 369	1.57 1.65	224 230	126 139	15.56 —	9.26 —	[20] [33, 34]

*For the nuclei ^{9}Be and ^{11}B only the $T_<$ branch was calculated in the COP variant.

TABLE VII. Total and energy-weighted photoabsorption cross sections in $1p$-shell nuclei with $N = Z$ (theory of Ref. 20): $MK(-x) \equiv MK(E_{1s})$.

Nucleus	b, F	Variant of calculation	Σ_0, MeV·mb	Σ_0/Σ_{TRK}	Σ_{-1}, mb
^{12}C	1.70	COP	303	1.68	12.6
^{14}N	1.70	COP	330	1.57	14.6
		MK(−12)	341	1.62	14.6
		MK	356	1.70	14.6
^{16}O	1.70	COP	386	1.61	16.7

nuclei in the middle and at the end of the $1p$ shell. The calculated integrated cross section exceeds the classical one by a factor of about 1.6 and is exhausted in the interval up to 35 MeV. The experimental data indicate that such exhaustion is realized over a much greater energy interval, of order 100 MeV.

The energy-weighted cross section and, in particular, the cross section

$$\sum_{-1}(E) = \int_0^E \sigma(E_\gamma)\, dE_\gamma / E_\gamma \tag{22}$$

is almost independent of model assumptions. The values of this quantity are given in Table V. For ^{7}Li, the theory gives a value for this quantity close to the measured one. With increasing atomic number of the nucleus, the theoretical value of Σ_{-1} begins to exceed the experimental value. The maximal excess is in the nucleus ^{16}O.

Concluding remarks

The cross sections calculated in both the BSM ($1\hbar\omega$) and the PFNS approach basically reproduce the observed energy dependence and the ratio of the intensities in the different regions of excitation energy of the nucleus. Practially all the experimentally observed gross structure of the cross section is explained. It is due to:

a) configurational splitting of the dipole resonance;

b) breakup of the "fouring" of the nucleons;

c) the isospin splitting of the resonance.

The theory basically reproduces the position of the main maximum to within a spread of 1–2 MeV but overestimates the cross section in almost the entire range of excitations up to 35 MeV.

Although spreading of the dipole resonance realized either by including all states in the $1\hbar\omega$-excitation band or in the PFNS approach led to a qualitatively important result—broadening of the localization region of the resonance—quantitative agreement with the experimental data is not always achieved. The next step necessary in this direction is to take into account states outside the $1\hbar\omega$-excitation band.

Completing the discussion of the gross structure of the dipole resonance, we note that the total-absorption cross sections do not provide a characteristic that at the present stage could discriminate between the various theoretical approaches. Much more informative are the partial transitions in the photodisintegration, to the discussion of which we now turn.

3. DECAY OF DIPOLE RESONANCE IN $1p$-SHELL NUCLEI. PHOTODISINTEGRATION PARTIAL CROSS SECTIONS

Basic features of the decay of the dipole resonance in $1p$-shell nuclei

If in the description of dipole photoabsorption a restriction is made to nucleon transitions in the $1\hbar\omega$-excitation band, then only three configurations [see (15)] are responsible for the formation of the resonance. Decay of the resonance through the nucleon channel can be realized in three ways:

$$1)\quad 1s^4 1p^{A-5} l \to 1s^4 1p^{A-5} + N(l). \tag{23}$$

The nucleon N is emitted with orbital angular momentum l equal to 0 or 2, and the final A–1 nucleus is formed in states with "normal parity": $\pi = (-1)^{A-1}$, these states being described by the configuration $1s^4\, 1p^{A-5}$

$$2)\quad 1s^4 1p^{A-5} l \to 1s^4 1p^{A-6} l + N(p). \tag{24}$$

The nucleon N is emitted with orbital angular momentum $l = 1$. This is the so-called "shaking off" of a $1p$ nucleon. As is shown by the experimental data[59] and calculations (see Sec. 5), this effect is small in the nuclei at the end of the $1p$ shell.

$$3)\quad 1s^3 1p^{A-3} \to 1s^3 1p^{A-4} + N(p). \tag{25}$$

The nucleon N is emitted with $l = 1$.

Since in the nuclei at the beginning of the $1p$ shell the dipole resonance is associated with a $1s \to 1p$ transition, the A–1 nucleus after emission of the p nucleon remains in a highly excited state with the configuration $1s^3\, 1p^{A-4}$ There then follows again a nucleon or cluster decay. Thus, in the disintegration of nuclei at the beginning of the $1p$ shell two or more particles or few-nucleon systems are formed with a high probability in the final state. This effect is sometimes called *star decay* of the resonance. It was discussed in Ref. 6. A cluster can also be emitted as a result of its direct knockout, as, for example, in the reactions $\gamma + {}^6\mathrm{Li} \to {}^3\mathrm{He} + {}^3\mathrm{H}$ or $\gamma + {}^7\mathrm{Li} \to {}^4\mathrm{He} + {}^3\mathrm{H}$, which were investigated in detail in Ref. 62.

Beginning with the nuclei ^{10,11}B, in which the $1s \to 1p$ transition no longer plays the decisive role in forming the dipole resonance, nucleon decay becomes predominant. The emitted nucleon carries away orbital angular momentum $l = 0$ or 2. With allowance for the presence of the subshells $1p_{1/2}$ and $1p_{3/2}$, the final A–1 nucleus after emission of the nucleon remains in states with the configuration $1s^4 1p_{3/2}^{A-n-5} 1p_{1/2}^n$. In nuclei with $A = 10$–12, the main configu-

TABLE VIII. Spectroscopic factors of $1p$ nucleon in the nuclei ^{12}C and ^{14}N and partial photodisintegration cross sections (references are given in square brackets).

Original nucleus	Final nucleus; E^*, MeV; J^π			Spectroscopic factor from the (p, d) reaction	Theoretical value of spectroscopic factor (Ref. 18). $p_{3/2}$	$p_{1/2}$	Partial photodisintigration cross section (experiment), MeV · mb
^{12}C	^{11}C	0	3/2$^-$	3.14 [63]	2.85	0	(77—88)% } (γ, p_0) 49 [116]
		2.0	1/2$^-$	0.54	0	0.75	(20—6)% } [76, 77]
		4.8	3/2$^-$	0.31	0.38	0	2% (γ, $p_{i\neq 0}$)5—8 [116]
	Sum			3.99 (4)	3.23+	0.75=3.98	
^{14}N	^{13}N	0	1/2$^-$	0.99 [64]	0	0.69	(γ, p) 9±1 [72]; (γ, n) 10,2 ±0,5 [71]
		3.51	3/2$^-$	0.30	0.14	0.02	(γ, p) 4±0,5 [72]
		7.39	5/2$^-$	1.51	1.86	0	(γ, p) 17 [82]
		8.92	1/2$^-$	0.75	0.61	0.05	
		9.52	3/2$^-$	0.99	1.15	0	
	Sum			4.56 (5)	3.76+	0.76=4.52	

ration forming the photonuclear resonance has $n = 0$. As a result of emission of the l nucleon, states of the A-1 nucleus with the configuration $1s^4 1p_{3/2}^{A-5}$ will be populated, the ground and low-lying levels of the A–1 nucleus corresponding to them. In the nuclei after the ^{12}C nucleus, $n \neq 0$, and as a result of the nucleon emission there will be populated states of the A–1 nucleus with the configuration $1s^4 1p_{3/2}^{A-n-5} 1p_{1/2}^n$. They lie quite high, sometimes above the threshold of subsequent breakup of the A–1 nucleus through the nucleon channel. Thus, population of excited states of the A–1 nucleus and emission of a secondary nucleon are characteristic of nuclei at the end of the $1p$ shell.

A characteristic feature of the photodisintegration reactions of the nuclei in the middle and at the end of the $1p$ shell is the preferred population of $1p_{3/2}$ hole states. A definition of hole states has already been given above [see (17)]. The value of the spectroscopic factor or the coefficient of fractional parentage indicates the extent to which a particular state of the A–1 nucleus is a hole state with respect to the ground state of the original nucleus A. Tables VIII and IX give the theoretical values of the spectroscopic factors calculated in Ref. 18. Experimentally, these factors are determined from data on reactions with quasielastic knockout of protons or on (p, d) reactions. Tables VIII and IX give the experimental values of the spectroscopic factors extracted from analysis of the (p, d) reaction.[63–67] The spectroscopic factors are normalized to make their sum equal to the number of neutrons in the $1p$ shell. This number is given in the brackets. It follows from the tables that the given levels almost exhaust the spectroscopic sum. The theory reproduces the observed features of the distribution of the spectroscopic system over the different levels.

The final columns of Tables VIII and IX give the partial photodisintegration cross sections, integrated over the photon energies, of the $1p$-shell nuclei. There is observed to be a correlation between the $1p$ spectroscopic factor and the partial cross section—the $1p$ hole states of the original nucleus are preferentially populated. The same correlation is found in the nuclei of the $2s$–$1d$ shell.[6] In this latter case, a systematic study has been made of the partial cross sections, and much factual material has been accumulated. It would be interesting to make similar systematic measurements for the $1p$-shell nuclei.

Fractional-parentage coupling of the dipole resonance of the nuclei ^{12}C and ^{14}N to levels of the hole nuclei (A–1)

As a result of photodisintegration of ^{12}C through the neutron channel there is preferential population of the ^{11}C ground state, since it exhausts an appreciable fraction of the spectroscopic strength of the ^{12}C ground state. But already in ^{14}N the ground and low-lying states are populated less intensively, since they have a $1p_{1/2}$-hole nature and have a weak fractional-parentage coupling to the main maximum of the dipole resonance (Table X). The table gives the results of the analysis of Ref. 31 on a complete basis of $1\hbar\omega$ configurations of the decay of the level $J^\pi T = 2^-\ 1$, which forms the maximum of the dipole resonance in ^{14}N ($\Sigma_0 = 78$ MeV · mb). Also reflected there is the fractional-parentage coupling of the resonance to the various states of the nuclei ^{13}N and ^{13}C (spectroscopic factors), together with the structure of the ^{13}N and ^{13}C states. The fractional-parentage coupling is strong to the levels $J^\pi = 5/2^-$ and $3/2^-$, which are situated in the region of excitation energies around 7 MeV; these are $1p_{3/2}$-hole levels. We note that the smallness of the spectroscopic factor describing the decay of the main maximum to the ground state of ^{13}N and ^{13}C leads to difficulties in its calculation—it is sensitive to many details in the structure of the nuclear states.

As follows from the results of the measurements, the ^{13}N–^{13}C ground state is populated in the photodisintegration of ^{14}N with a greater probability than follows from the theory. According to the measurements, the fraction of transitions to the ground state is about 15%,[71,72] whereas the theory gives only about 6%. It should here be noted that the description of the transitions to the ground state of the daughter nucleus is here an open problem of the theory. A detailed discussion of the decay properties of the resonance in ^{12}C and ^{14}N will be given in Sec. 4.

TABLE IX. Spectroscopic factors of $1p$ nucleon in the nuclei ^{15}N and ^{13}C and partial photodisintegration cross sections (references are given in square brackets).

Original nucleus	Final nucleus; E^*, MeV; $J^\pi T$			Spectroscopic factor from the (p, d) reaction	Theoretical value of spectroscopic factor (Ref. 18)		Partial photodisintegration cross section (experiment), mb · MeV (%)
					$p_{3/2}$	$p_{1/2}$	
^{15}N	^{14}C	0	0^+1	—	0	0.84	22 [69]
		7.01	2^+1		2.39	0	7.9 [70], 52±7 [75]
		8.32	2^+1				
		10.7	1^+1		1.50	0	15±3 [75]
	Sum				3.89+0.84=4.73		
	^{14}N	0	1^+0	1.27 [65]	0.03	1.43	18 [68]
		2.31	0^+1	0.50	0	0.42	8.6
		3.95	1^+0	0.60	0.65	0.05	8.3 [70]
		7.03	2^+0	1.02	1.25	0	7.9
		9.17	2^+1	0.49	1.19	—	—
		10.43	2^+1	0.39		0	—
	Sum			5.08 (6)	3.87+1.90=5.77		
^{13}C	^{12}B	0	2^+1	—	2.02	0	(14%) [59]
		0.95	0^+1		0	0.19	(17%) [59]
			1^+1		1.20	0	
	Sum				3,22+0,19=3,41		(31%) [59]
	^{12}C	0	0^+0	0.82 [66, 67]	0	0,61	(20%) [59], 23 [73]
		4.44	2^+0	1.19	1,12	0	(5%) [59]
		12.7	1^+0	0.62	0,66	0	— [59]
		15.1	1^+1	0.56	0,60	0	(17%) [59]
		16.1	2^+1	1.03	1,01	0	(27%) [59]
	Sum			4.12 (5)	3.39+0.61=4.00		(69%) [59]

TABLE X. Spectroscopic factors calculated in a complete basis of $1\hbar\omega$ excitations for decay of the main peak of the giant dipole resonance in ^{14}N (2^- 1, $E = 22$ MeV) to ^{13}C and ^{13}N states and integrated partial cross sections: $\int\sigma(E_\gamma)dE_\gamma = 78$ mb · MeV.[31]

J^π	E^*, MeV		Neutron spectroscopic factors[18] determining the structure of the states of the nuclei ^{13}C and ^{13}N		Orbital angular momentum l_j of emitted nucleon	Spectroscopic factors determining the decay of the main maximum[31]	Integrated partial cross sections, mb · MeV	
	^{13}C	^{13}N	$p_{1/2}$	$p_{3/2}$			^{13}C	^{13}N
1/2−	Ground		0,69	0,005	$d_{5/2}$	0,002	0,9	0,9
					$d_{3/2}$	0,020	8,0	7,3
3/2−	3.68	3,51	0,025	0,14	$d_{5/2}$	0,002	0,7	0,6
					$d_{3/2}$	0,005	1,3	1,1
					$2s_{1/2}$	0,001	0,2	0,2
5/2−	7.55	7,40	0,015	1,86	$d_{5/2}$	0,129	18,0	10,4
					$d_{3/2}$	0,010	1,4	0,8
					$2s_{1/2}$	0,015	5,2	4,5
1/2−	8.86	8,92	0,055	0.615	$d_{5/2}$	0,033	3,1	1,2
					$d_{3/2}$	0,035	3,3	1,3
3/2−	9,90	9,52	0,005	1.15	$d_{5/2}$	0,164	5,0	0
					$d_{3/2}$	0,001	0	0
					$2s_{1/2}$	0,002	0,5	0,2
Sum			0,79	3,77		0.419	47,6	28,5

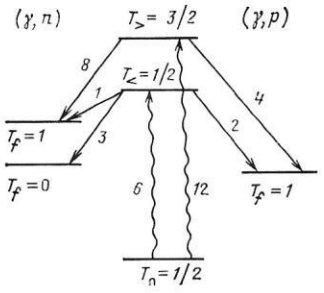

FIG. 10. Decay scheme of photonuclear resonance in nuclei with $T_0 = 1/2$ with indication of the transition intensities obtained from the geometrical factors.

Fractional-parentage coupling of the dipole resonance in the nuclei ^{13}C and ^{15}N to the levels of the final nuclei

The decay scheme of the odd nuclei of the $1p$ shell is shown in Fig. 10. The scheme shows, in relative units, the geometrical factors that determine the excitation intensities of both isospin branches of the resonance and the geometrical factors that determine the intensity of population of the various isospin groups of levels of the final $A-1$ nucleus. These factors do not take into account the influence of the penetrability of the barrier (Coulomb and centrifugal). The relative units are chosen to make the weakest $T_<$ decay branch through the neutron channel to the $T_f = 1$ levels correspond to one intensity unit. The barrier penetrability transforms the relative quantities given in the scheme, particularly for decay of the $T_<$ branch to the $T_f = 1$ levels, since in this case the energy release is low. And in the odd nuclei ^{13}C and ^{15}N the fraction of transitions to the ground state of the nuclei ^{12}C and ^{14}N, respectively, is small, since they are coupled, not to the complete photonuclear resonance, but only to its $T_<$ branch, provided, of course, that the isospin mixing of the two branches is small. Indeed, the transitions to the ground and low-lying states of the $A-1$ nuclei with isospin $T_f = 0$ make it possible to separate the $T_<$ branch of the resonance.

The pygmy resonance also has a fractional-parentage coupling which is stronger to the excited states of the final $A-1$ nucleus than to the ground state (Tables XI and XII). Because of this, the theory predicts that the ground state of ^{12}C will be less strongly populated in the ^{13}C(γ, n) reaction than the state $J^\pi T = 2^+ 0$, $E = 4.4$ MeV. Thus, in accordance with Ref. 29, $\Sigma_0(\gamma, n_1)/\Sigma_0(\gamma, n_0) = 3$; according to Ref. 15, this ratio is 1.74; and only according to Ref. 17 is it 0.93. The first result is obtained in the BSM and the last two in the CSM. The experimental data are also contradictory: 0.58 in Ref. 73, 0.35 in Ref. 74, and 0.25 in Ref. 59. However, in all three cases the ratio does not exceed unity. A detailed discussion of the decay properties of the resonance in ^{13}C and ^{15}N will be given in Sec. 5.

Photoproton and photoneutron decays

Experimental data on the integrated cross sections of the photoproton and photoneutron channels of disintegration of the $1p$-shell nuclei are given in Table XIII. For nuclei with $T_0 = 0$, the (γ, p) and (γ, n) reactions lead to population of the levels of the mirror nuclei with $T = 1/2$. The spectroscopic factors that determine the coupling of the resonance to the levels to which the decay takes place are the same in the two channels. The deviation from symmetry arises because of the lower thresholds of proton separation and, secondly, because of the Coulomb barrier in the proton channel. According to the calculations, the first factor is more important than the second, and this raises the probability of proton decay of the photonuclear resonance in the considered nuclei above that of the neutron decay (see Sec. 4 below).

However, the relationship between the proton and neutron photodisintegration channels of the $1p$-shell nuclei depends not only on the ratio of the probabilities of the primary nucleons but also on the yield of secondary nucleons emitted as a result of decay of the highly excited levels of the A–1 nucleus. Thus, in ^{14}N only 15% of the total-absorption cross section is associated with population of discrete states of the nuclei ^{13}N and ^{13}C.

For nuclei with $T_0 \neq 0$, the neutron type of photodisintegration is predominant. The $T_>$ branch of the dipole resonance decays only to states of the final nuclei with isospin $T_f = 1$. The predominance of the neutron decay in this case is associated with the geometrical factors, given in Fig. 10.

TABLE XI. Spectroscopic factors for the strongest resonances corresponding to the ^{13}C(γ, n) ^{12}C channel.[29]

Quantum numbers of states forming the resonance		Σ, MeV · mb	State of final nucleus		Spectroscopic factors		
$J_i^\pi T_i$	E^*, MeV		$J_f^\pi T_f$	E_f^*, MeV	$1d_{5/2}$	$2s_{1/2}$	$1d_{3/2}$
1/2+ 1/2	15.6	10	0+0	0	—	0,010	—
			2+0	4,44	0,514	—	0,051
3/2+ 1/2	19.2	12	0+0	0	—	—	0,007
			2+0	4,44	0,008	0,002	0,002
			1+0	12,7	0,286	0,001	0,001
3/2+ 3/2	24,9	52	1+1	15,1	0,095	0,001	0,050
			2+1	16,1	0,237	0,022	0,010

TABLE XII. Spectroscopic factors for the strongest resonances corresponding to the $^{15}N(\gamma, n)^{14}N$ channel.[33,34]

Quantum numbers of states forming the resonance		Σ, MeV · mb	States of final nucleus		Σ, partial, MeV · mb	Spectroscopic factors	
$J_i^\pi T_i$	E^*, MeV		$J_f^\pi T_f$	E_f^*, MeV		2s	1d
3/2+1/2	15.4	12.6	1+0	0	12.2	0.03	0.14
	22.7	25.2	1+0	0	6.8	0	0.10
			2+0	7.03	6.9	0.1	0.24
			1+0	3.95	3.6	0.02	0.04
1/2+1/2	17.9	11.0	1+0	0	1.3	0.01	0
			1+0	3.95	4.1	0.01	0.02
3/2+3/2	21.3	20.8	0+1	2.3	4.6	0	0.06
			2+1	9.2	4.5	0.04	0.67
				10.4			
	24.4	95.0	0+1	2.3	18.2	0	0.05
			2+1	9.2	22.6	0.02	0.14
				10.4			
	26.2	13.4	2+1	9.2	5.5	0.01	0.37
				10.4			
1/2+3/2	23.6	41.5	2+1	9.2	15.7	0	0.73
				10.4			
	25.4	10.2	1+1	13.7	2.7	0.33	0.04

The $T_<$ branch can decay either to levels with $T_f = T_0 - 1/2$ or to levels with $T_f = T_0 + 1/2$ of the final nucleus. The low-lying region of the $T_<$ branch decays predominantly to states with $T_f = T_0 - 1/2$ through the neutron channel. This question will be discussed in somewhat more detail in Sec. 5 for the example of the ^{15}N nucleus.

TABLE XIII. Photoneutron and photoproton disintegration cross sections and nucleon separation energies.

Nucleus	E_{max} or $E_1 - E_2$, MeV	$\Sigma_0(n)$, MeV · mb	$\Sigma_0(p)$, MeV · mb	ε_n, MeV	ε_p, MeV	References
^7Li	23	56	27	7.3	10.0	[115, 112]
^9Be	18—26	13	—	1.7	≈ 16.9	[53]
	17—40	—	25			[112]
^{11}B	35	69	—	11.5	11.2	[54]
^{13}C	30	95	55	4.9	17.5	[60]
	28	85	36			[56]
^{15}N	30	90	70	10.8	10.2	[60]
^{10}B	35	81	—	8.4	6.6	[54]
^{12}C	30	42	72	18.7	16.0	[60]
	29	—	56			[116]
^{14}N	30	99	15	10.6	7.6	[60]
^{16}O	30	48	87	15.7	12.1	[60]

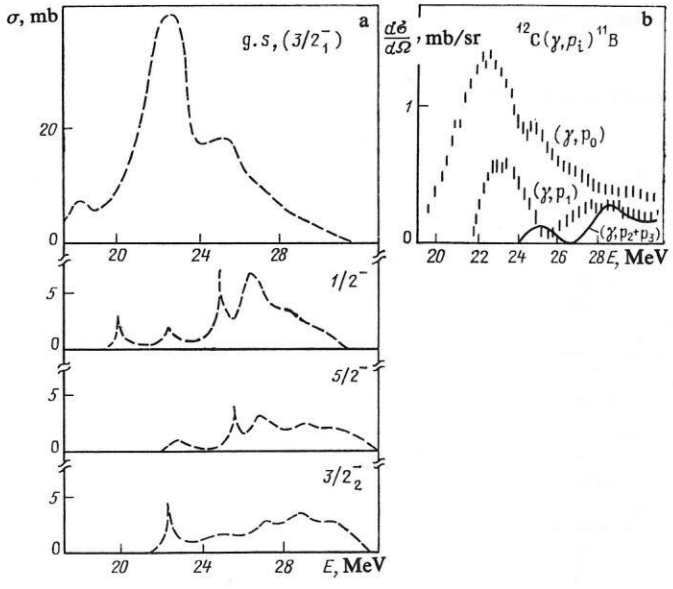

FIG. 11. Partial photodisintegration cross sections of the ^{12}C nucleus: a) calculation of Ref. 37; b) experimental data of Ref. 77.

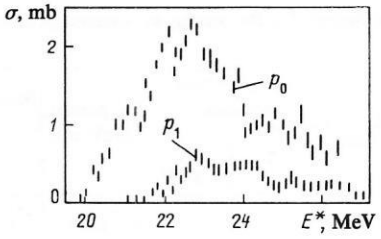

FIG. 12. Results of measurement of the ^{12}C$(e, e'p)$ reaction[80]: $\theta_1 = 40°$, $\theta_p = 120°$.

4. PARTIAL TRANSITIONS IN THE NUCLEI IN THE MIDDLE AND AT THE END OF THE 1*p* SHELL WITH $T_0 = 0$

The nucleus ^{12}C

Experimental data on the partial cross sections for ^{12}C photodisintegration,[76,77] and also the results of calculations obtained in various theoretical approaches, are given in Fig. 11 and in Table XIV. The first two columns, which relate to the calculations, correspond to the PFNS approach[35,37] but to different variants of the residual nucleon-nucleon interaction and the single-particle energies.

As follows from the experimental data, the ^{12}C$(\gamma, p_0)^{11}$B cross section is characterized by two clear maxima: $E^* = 22$–23 MeV and $E^* = 25$–26 MeV. In the inverse ^{11}B$(p,\gamma_0)^{12}$C reaction, a similar structure of the energy dependence of the cross section was obtained.[78,79]

The results of the measurements of Refs. 76 and 77 differ in the estimate of the ratio of the contributions to the total ^{12}C photodisintegration cross section of the transitions to the ground $(3/2)_1$ state and the first excited $(1/2)_1$ state of the final nucleus (see Table XIV). The photonuclear data on ^{12}C are significantly augmented by the results of the measurements of Ref. 80 of the ^{12}C$(e, ep)^{11}$B reaction cross section; these measurements fixed coincidences of an electron and a proton (Fig. 12) under conditions when the reaction proceeds predominantly through excitation of the dipole resonance. The experimental data on the $(e, e'p_0)$ and $(e, e'p_1)$ cross sections basically confirm the photonuclear data obtained in Ref 77. The angular correlations in the ^{12}C$(e, e'p_0)$ and $^{12}C\,(e, e'p_1)$ reactions indicate[80] that at nuclear excitation energies around 25 MeV the importance of the $(e, e'p_1)$ reaction increases. The angular distribution of the emitted p_0 and p_1 protons is characterized by a larger value of the coefficient a_2 (~ -0.5) in the Legendre-polynomial expansion, this corresponding to preferential emission of protons with angular momentum $1 = 2$.

The conditions under which the experiment of Ref. 80 were made were such that the electrodisintegration of ^{12}C was determined by the $C\,1$ and $E\,1$ multipoles. The assumption that the second maximum in the total ^{12}C photodisintegration cross section is due to the contribution of $E\,2$ transitions is not confirmed by the results of Refs. 79 and 80. It follows from these measurements that the fraction $\Sigma_0(E\,2)$ in the total cross section does not exceed 5%. Thus, one gets the impression that in reality the fraction of the cross section of the (γ, p_0) reaction in the total (γ, p) cross section is less than follows from the results of the measurements made in Ref. 76. However, the recent data of investigations of the ^{12}C$(\gamma, p_0)^{11}$B reaction[116] confirm the result of Ref. 76.

According to the data of Refs. 76 and 77, the cross sections of partial transitions to excited ^{11}B states higher than the first do not contradict each other. However, the accuracy of these measurements is as yet low. In Ref. 77, the contributions of the transitions to the second and third excited states were not separated. We note that the total cross section has a minimum at $E_\gamma \sim 26$ MeV.

The results of calculations of the partial ^{12}C photodisintegration channels are given in Fig. 11 and in Table XIV. Figure 11 reflects the results of the calculation of Ref. 37 with Gillet-1 forces (see Table IV). An analogous calculation with Rosenfeld forces leads to a raising of the relative probability of the transitions to the excited states of the final nu-

TABLE XIV. Partial ^{12}C photodisintegration cross sections (references are given in square brackets).

Levels of final ^{11}B nucleus		Experiment		Theory			
J_n^π	E^*, MeV	$\frac{\Sigma(\gamma, p_i)}{\Sigma(\gamma, p_{tot})}$, %		$\frac{\Sigma_i}{\Sigma_{tot}}$, %			
		[76]	[77]	[37]	[37]	[36]	[81]
$(3/2^-)_1$	0	88.4±10	76.9±1.1	75	55	68	80
$(1/2^-)_1$	2.12	5.4±10	20.8±0.6	13	23		9
$(5/2^-)_1$	4.46	1.4±15	2.3±0.2	5	7	32	3
$(3/2^-)_2$	5.02	2.0±15		7	14		7

cleus. It is characteristic that the results of the calculation for the total photodisintegration cross sections for all the employed variants of the residual nucleon-nucleon interaction forces given in Table XIV are practically the same. The partial cross sections represent the characteristic of the photonuclear reactions most sensitive to the parameters of the model calculations.

The cross section of the transition to the ground state is well reproduced by the calculations in the PFNS approach.[37] The ratio of the cross sections at the peaks at $E_\gamma = 22$ MeV and $E_\gamma = 25.5$ MeV is approximately 2:1, which corresponds to the observed value.[78,79] According to the calculation of Refs. 35 and 37, the main contribution to the wave function of the state forming the main peak of the dipole resonance is made by the component $|(3/2)_1\ 1d_{5/2}\rangle$. However, 15–20% of the contribution to the main maximum of the total cross section is made by the $|(3/2)_2\ 1d_{5/2}\rangle$ configuration above the third excited state of the $A = 11$ nuclei. In the wave function of the state forming the second maximum ($E^* \sim 25.5$ MeV), an important part is played by the $|(3/2)_1\ 1d_{3/2}\rangle$ configuration.

The transition to the second excited state of ^{11}C and ^{11}B is interesting in that the corresponding levels are hole levels, not with respect to the ^{12}C ground state, but with respect to the level $J^\pi T = 2^+\ 0$ ($E^* = 4.4$ MeV). Such transitions are the result of coupling of the dipole and quadrupole vibration modes in ^{12}C.

Analysis of the partial cross sections in ^{12}C shows that the use of a large basis to describe the decay characteristics of the dipole resonance is a necessary condition if the main features of photodisintegration are to be reproduced. A model that includes continuum states, the CSM, but constructed on a restricted basis, has great difficulties in interpreting the experimental data. A model that takes into account a large number of configurations reflects the observed picture much more fully.

On the other hand, analysis of the partial characteristics has revealed that the results are critically sensitive to the structure of the wave functions of the individual resonances, which to a large degree depend on the nature of the residual nucleon-nucleon interaction and the single-particle energies. In the light nuclei, there is still a large arbitrariness with regard to both the choice of the interaction and the choice of the single-particle energies. Work on the unification of this part of the problem is needed.

The theories that use a large basis have not yet been able to overcome the difficulties associated with the excessive concentration of the resonance in the region of the main maximum; to an even greater degree this introduces difficulties in the description of the decay properties.

It is possible to analyze quantitatively the relative but not the absolute decay characteristics, and this greatly restricts the possibilities of deep testing of the theory. Despite all these difficulties, as we have seen, the partial characteristics are, even at the present state of the art, a more delicate probe of the dipole-resonance structure and make it possible to test many predictions of the theory much more deeply, though as yet on a semiquantitative basis.

The nucleus ^{14}N

The main results of the investigations (Refs. 20, 31, 39, 69, 71, 72, and 82–90) of the photodisintegration of ^{14}N are

TABLE XV. Partial photodisintegration cross sections of the nucleus ^{14}N (references are given in square brackets).

Reaction	State of final nucleus, $J^\pi T = 1/2$, E, MeV	Integrated partial cross section, MeV · mb (%)			
		Experiment	Theory		
			[31]	[39]	[20]
^{14}N (γ, p) ^{13}C	1/2$^-$, 0	9 [72]; 11 [87]; 20 [82]	19 (5.3)	(8)	(6)
	1/2$^+$; 3.09	2 [86]			
	3/2$^-$; 3.68	2,5 [86]; 7 [84]	13 (3.8)	(14.2)	(9.3)
	5/2$^+$; 3.85	1 [86]			
	5/2$^-$; 7.55	17 [82]	63 (18)	(12.8)	(16.3)
	1/2$^-$; 8.86		20 (5.8)	(9.8)	(4.2)
	3/2$^-$; 9.90		26 (7.5)	—	—
	3/2$^-$; 11.85	5 [82]	8 (2.4)	(4.8)	(12.3)
	Σ (γ, p)				
^{14}N (γ, n) ^{13}N	1/2$^-$, 0	10,2 [71]; 20 [82]	16 (4.6)	(4.9)	(5.0)
	1/2$^+$; 2.37	2,2 [86]			
	3/2$^-$; 3.51	6 [82]	11 (3.2)	(10.8)	(7.6)
	5/2$^-$; 7.38		40 (11.6)	(10.4)	(10.8)
	1/2$^-$; 8.92		12 (3.4)	(8.1)	(2.0)
	3/2$^-$; 9.48		13 (3.8)	(4.4)	(4.3)
	Σ (γ, n)	99 [60]			
^{14}N (γ, d) ^{12}C + ^{14}N (γ, pn) ^{12}C	0$^+$, 0	—	158 (44)		
	2$^+$; 4.44	11 [86]	128 (35)		
	α-unstable levels	36 (11) [88]	21 (5.8)		

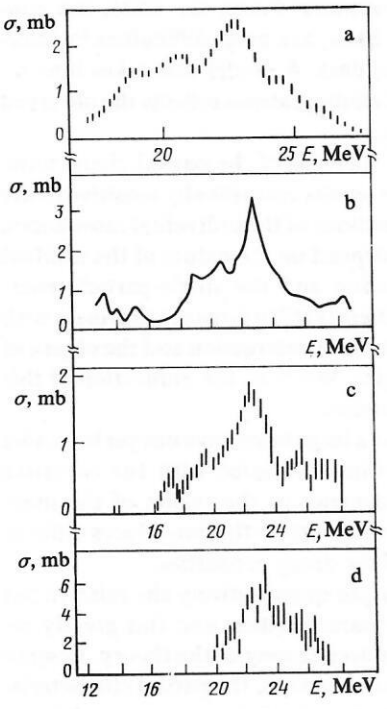

FIG. 13. Results of measurements of the partial cross sections in ^{14}N; a) (γ, n_0) (Ref. 71); b) (γ, p_0) (Ref. 90); c) $(\gamma, p_{3.68})$ (Ref. 90); d) $(\gamma, p_{7.55})$ (Ref. 90).

given in Table XV and Figs. 13 and 14. The theory reproduces the energy dependence of the (γ, p_0) cross section, but the maxima, as in the total-absorption curve (Fig. 4), are displaced somewhat to lower energies.

The large number of partial disintegration channels is

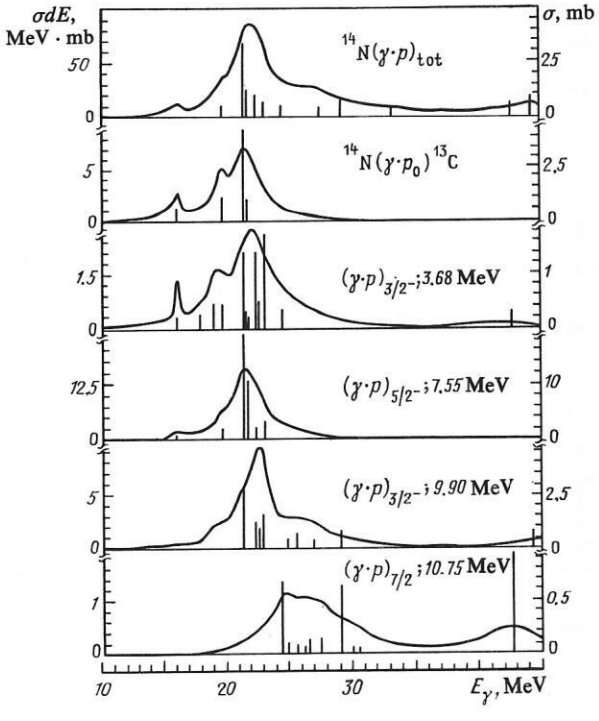

FIG. 14. Partial cross sections of ^{14}N photodisintegration according to BSM($1\hbar\omega$) theory.[31]

due to the nature of the spreading of the $1p$-hole states (see Table VIII). Their large width of spreading is due to the approximate realization of supermultiplet structure in this nucleus. The lower group of transitions is associated with the conservation of the "touring" of the nucleons, while the upper group arises from its breakup. The fractions of transitions to the ground states of ^{13}C and ^{13}N are nearly equal and are about 15% of the total cross section. The energy dependences of the (γ, p_0) and (γ, n_0) cross sections are also similar.

According to the measurements of Ref. 90, $\Sigma(\gamma, p_{7/55})/\Sigma(\gamma, p_0) \gtrsim 2$, this being lower than the result of the calculation in the variant CAL BSM($1\hbar\omega$).[31] Calculations in the variant COP BSM($1\hbar\omega$) (Ref. 20) and in the PFNS approach[39] give lower values. The sensitivity of the (γ, p_2) and (γ, n_2) cross sections to the choice of the model parameters is due to the fact that the corresponding ^{13}C and ^{13}N states are not hole states with respect to the ^{14}N ground state.

Analysis of the angular distributions[72,90] shows that in the (γ, p_0) reaction the $1p_{1/2}^{-1}2s_{1/2}$ and $1p_{1/2}^{-1}1d_{3/2}$ configurations are predominant, primarily the latter at $E_\gamma > 23$ MeV. In the (γ, p_2) cross section, transitions from the $1p_{3/2}$ subshell are predominant.

In only half the cases does the theory associate the population of the ^{13}C and ^{13}N ground states with decay of the main maximum of the dipole resonance. The emitted nucleon has in this case the quantum numbers $d_{3/2}$ (see Table X). The population of the $5/2^-$ level is due primarily to decay of the main maximum and emission of a $d_{5/2}$ nucleon.

All the excited states of ^{13}N and all except the first three ^{13}C states populated as a result of decay of the resonance in ^{14}N are unstable with respect to emission of a nucleon. The intensity of the population of such states is high-more than 60%, as follows from the calculations of Refs. 31 and 39. As a result, the integrated cross section $\sigma(\gamma, n_{tot})$ appreciably exceeds the cross section for the emission of primary neutrons.

The (γ, d), (γ, α), and $(\gamma, 2\alpha)$ cluster decays from the dipole-resonance states for which $T = 1$ to the ground states of the nuclei with A-2 and A-4, $T = 0$ are forbidden by isospin. The fraction of the primary (γ, α) reaction is not more than 2% of the total cross section.[88,89] Among the α channels, the most important is $(\gamma, pn, 3\alpha)$.

The decay properties of the dipole resonance in ^{14}N were calculated in Refs. 20, 31, and 39. The partial cross sections to the ground state of the $A = 13$ nuclei obtained in calculations using a complete $1\hbar\omega$ basis (Fig. 14) reproduce rather well the experimental data in the region from the threshold to $E_\gamma \lesssim 25$ MeV. Transitions from the region $E_\gamma > 25$ MeV are not reproduced in the (γ, n_0) and (γ, p_0) calculations.

We now turn to the energy spectra of the nucleons. Figure 15 shows the result of a calculation of the proton energy spectrum in the PFNS approach[39] (histogram). The normalization is chosen to make the experimental data pass through the histogram at the point of its maximum. The theory reproduces the behavior of the energy dependence from $E_p = 4$ MeV onward. At the same time, Fig. 15 reveals

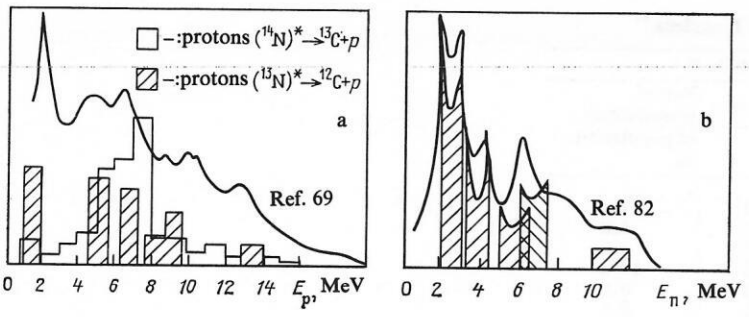

FIG. 15. a) Spectra of photonucleons in the ^{14}N(γ, p_{tot}) reaction[39,69]; b) spectrum of secondary neutrons in ^{14}N photodisintegration.[39,82]

the difficulties of the theory too—the softest part of the spectrum, which is most probably associated with pre-equilibrium and equilibrium processes, is depleted. There is a similar situation in the neutron channel.

As already noted, the contribution of secondary decay in ^{14}N photodisintegration is large. We note an interesting effect which arises in connection with this in the nucleon spectrum. The shape of the spectral peaks of the secondary nucleons (nucleons from de-excitation of the intermediate nucleus) feels the effect of the nature of the angular distribution of the primary photonucleons. The anisotropy of their emission due to the Doppler shift leads to a splitting of the peaks. Figure 15b illustrates[39] the effect by the example when allowance is made for the angular distributions of the primary protons in the spectral curve of the neutrons. If ^{13}C is formed in the states $5/2^-$ and $1/2^-$, then the probability for emission of d protons is greater than that for s protons, and this predetermines a splitting of the peaks of the secondary neutrons.

Concluding the discussion of the photodisintegration of ^{14}N, we note that the rich spectrum of partial transitions in this nucleus has made it possible to test quite thoroughly the capabilities of the theoretical method. Basically, the theory correctly describes the gross structure of the partial cross sections. As the next step in the systematic analysis of the partial cross sections it appears important to make a theoretical analysis of the angular distributions using the same basis of $1\hbar\omega$ excitations. Also incomplete as yet is the experimental study of all strong transitions. Moreover, the absolute values of the measured cross sections differ in a number of cases rather strongly, and this, of course, makes an unambiguous interpretation difficult.

The nucleus ^{10}B

In the decay of dipole excitations of the ^{10}B nucleus solely as a result of the ^{10}B$(\gamma, p_0)^9$Be reaction there arises a state stable with respect to further decays. All the remaining partial channels of ^{10}B photodisintegration lead to many-step decays, for example, ^{10}B$(\gamma, n_0)^9$B, ^{9}B $\rightarrow$ ^{8}Be $+ p$, ^{8}Be $\rightarrow 2^4$He. As a result, the final products of photodisintegration through all channels except (γ, p_0) will be two α particles, a proton, and a neutron. Except for the (γ, p_0) channel, there are no experimental data on any of the partial channels of the ^{10}B photodisintegration. The cross section and angular distributions in the ^{9}Be$(p, \gamma_0)^{10}$B capture reaction[91] are given in Fig. 16. The results of calculation of the partial ^{10}B photodisintegration channels in the PFNS approach[41] are given in Fig. 16 and in Table XVI. The total photodisintegration cross section in this calculation and the $\sigma(\gamma, n_{tot})$ data[54] were given in Fig. 5. The appreciable width of the region of the dipole excitations of the ^{10}B nucleus is associated with the spreading of the states of the final nuclei over a wide interval of excitation energies.

The distributions of the partial cross sections of the (γ, p_i) and (γ, n_i) reactions are very similar. The main maxima of the dipole excitations of the ^{10}B nucleus are formed by configurations constructed on excited states of the daughter nuclei, among which states the $7/2^-$ state plays the most important part. Transitions to these states of the daughter nuclei form the maximum of the cross section at $E \approx 20$ MeV. According to the data of the calculation, the transitions to the ^{9}Be ground state occur mainly from the $4^- T = 1$ excited state with $E^* = 11$ MeV. However, comparison of the theoretical curve with data on the capture reaction

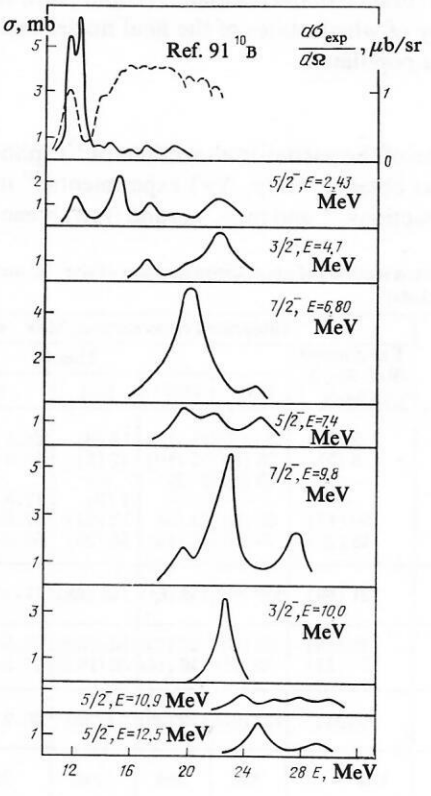

FIG. 16. Partial (γ, p_i) channels in ^{10}B photodisintegration: theory of Ref. 41; experiment of Ref. 91; the upper figure shows $\sigma(\gamma, p_0)$.

TABLE XVI. Partial probabilities of photodisintegration of the ^{10}B nucleus.[41]

Reaction (γ, n)			Reaction (γ, p)		
States of the ^{9}B nucleus		Partial probabilities of population, %	States of the ^{9}Be nucleus		Partial probabilities of population, %
E, MeV	J		E, MeV	J	
g. s	3/2	6.7	g. s	3/2	7.7
2.36	5/2	4.9	2.43	5/2	4.8
4.70	3/2	4.0	4.70	3/2	4.0
7.00	7/2	10.9	6.80	7/2	10.6
7.4	5/2	5.8	7.4	5/2	5.8
9.8	7/2	8.1	9.8	7/2	8.1
10.0	3/2	1.9	10.0	3/2	2.0
10.9	5/2	2.6	10.9	5/2	2.7
12.5	5/2	2.8	12.5	5/2	2.9
$\Sigma(\gamma, n)$		48.1	$\Sigma(\gamma, p)$		51.9

shows that the calculation underestimates the transitions to the ground states of the daughter nuclei from the region of excitation energies 13–20 MeV.

5. PHOTODISINTEGRATION OF NUCLEI IN THE MIDDLE AND AT THE END OF THE 1p SHELL WITH $T_0 \neq 0$

The photodisintegration of nuclei in the middle and at the end of the 1p shell with $T_0 \neq 0$ (^{13}C, ^{15}N, ^{11}B, ^{14}C) takes place with the excitation of two branches of the dipole resonance: $T_< = T_0$ and $T_> = T_0 + 1$. The decay of the low-energy part of the $T_<$ branch—the pygmy resonance—takes place to the ground and low excited states of the A–1 nucleus exclusively through the neutron channel with population of $T_f = T_0 - 1/2$ states. In the region of excitation energies 22–35 MeV, the $T_>$ branch of the resonance is dominant, as a result of the decay of which states of the final nuclei with $T_f = T_0 + 1/2$ are populated.

The nucleus ^{13}C

The distribution of the partial cross sections of ^{13}C photodisintegration was obtained in (γ, $N\gamma'$) experiments,[59] in radiative capture reactions,[73] and in (γ, n_0) and (γ, n_1) reactions.[74] The cross sections of photoneutron and photoproton disintegration were measured with the greatest accuracy in Refs. 55 and 56. A theoretical investigation of the partial cross sections of ^{13}C photodisintegration has been made in both the BSM[20,29,38] and the CSM.[15,17] There have been calculations on a complete basis using not only purely central forces of the residual interactions[29] but also the variant of the MK forces.[20,50] The results of the investigations of the partial channels of ^{13}C photodisintegration are given in Table XVII. The energy distribution of the partial cross sections in accordance with the data of Refs. 59 and 74 is compared with the results of the calculation of Ref. 29 in Fig. 17.

A characteristic feature of the ^{13}C photodisintegration is the complicated structure of the cross section of the (γ, n_0) reaction. Besides several maxima in the region of the pygmy resonance, this cross section has a peak at $E \simeq 20$ MeV and makes an appreciable contribution to the region of excitation energies $E > 30$ MeV.[59] The calculations made in the BSM lower the fraction of the (γ, n_0) channel in the total photodisintegration cross section; allowance for the continuum somewhat improves the agreement with experiment. Underestimation of the transitions to the ground state of the ^{12}C

TABLE XVII. Partial cross sections of photodisintegration of the ^{13}C nucleus (references are given in square brackets).

Reaction	E* of nucleus with A = 12, MeV	$J^\pi T$	Integrated cross section, MeV · mb (%)					
			Experiment (Ref. 59); Σ_γ ⩽38 MeV	Theory				
				[29] *	[20] *	[38]	[15]	[17]
(γ, n)	0	0+0	35 (20)	8 (2,5)	11 (3,4)	17 (8)	28.8 (11.9)	39 (15)
	4.44	2+0	8 (5)	26 (8)	32 (10)	17 (8)	50.0 (20.6)	37 (14)
	10.3	0+0	—	13 (4)	6 (2)	—	—	—
	12.7	1+0	—	—	—	7 (3)	17.5 (7.3)	10 (4)
	15.11	1+1	30 (17)	26 (8)	25 (8)	52 (24)	27.5 (11.3)	39 (15)
	16.11	2+1	48 (27)	43 (13)	44 (14)	54 (25)	50.0 (20.6)	68 (26)
	$\Sigma(\gamma, n)$		121 (69)	208 (63)	196 (61)	146 (68)	174 (72)	193 (74)
(γ, p)	0	1+1	25 (14)	26 (8)	22 (7)	34 (15.5)	27.5 (11.2)	24 (9)
	0.95	2+1	30 (17)	36 (11)	46 (14)	36 (16.5)	41.2 (17)	45 (17)
	$\Sigma(\gamma, p)$		55 (31)	122 (37)	122 (38)	70 (32)	68.7 (28.2)	69 (26)
	Σ		176	330	318	216	242.5	262

*Data on the main decay channels of the giant dipole resonance are given.

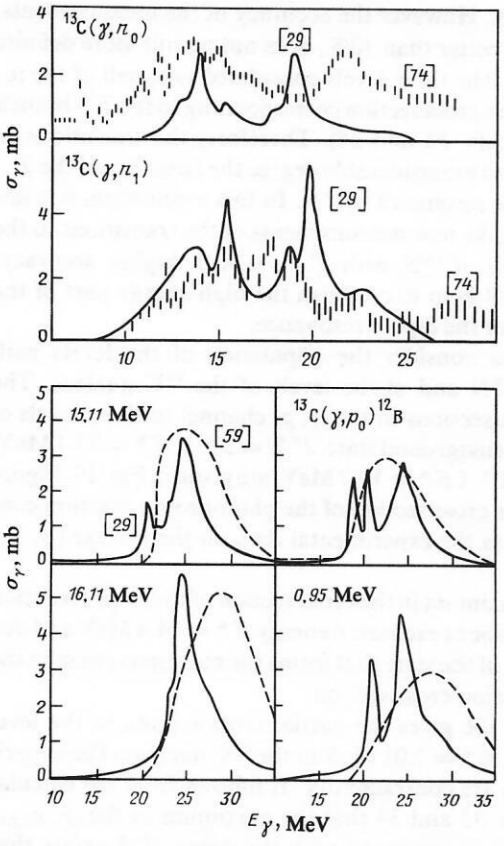

FIG. 17. Partial cross sections of ^{13}C photodisintegration: theory of Ref. 29 (continuous curves) and experiment of Refs. 59 and 74 (references are indicated in square brackets).

nucleus from the region of high excitation energies is a shortcoming common to all the theoretical calculations.

The partial cross section of the $^{13}C(\gamma, n_1)^{12}C(2^+ T=0)$ reaction reflects the probability of excitation of quadrupole vibrations of the core in the photodisintegration of the ^{13}C nucleus. The experimental estimates of the ratio of the cross sections $\sigma(\gamma, n_0)$ and $\sigma(\gamma, n_1)$ differ by more than a factor 2 (see Sec. 3). Allowance for channel coupling through the continuum strongly raises the probability of the (γ, n_1) channel and predicts[15] a large contribution of the channel to the region of the main maximum of the giant dipole resonance. Calculations in the BSM lead to a more realistic picture. For the distribution over the energy of the (γ, n_1) cross section there is, according to the data of Ref. 74 and the results of the calculations of Ref. 29, a characteristic spread over an interval $E = 12$–22 MeV with several maxima in the cross section (Fig. 17). However, according to the $(\gamma, N\gamma')$ data,[59] the cross section in this channel is concentrated at energies 11–16 MeV. Consistency of the results on the $C(\gamma, n_1)$ cross section requires a more careful investigation of this photodisintegration channel for a wide range of excitation energies.

A characteristic feature of the photodisintegration cross sections of the ^{13}C nucleus is the narrow peak at excitation energy 20 MeV. The BSM[29,38,57] reproduces this peak well, interpreting it as an excitation with $T = 1/2$, although in some calculation variants (PFNS with Rosenfeld mixing forces[38,58]) part of the dipole strength at this maximum is attributed to the $T = 3/2$ branch. According to the calculations of Ref. 29, the decay of the dipole excitations concentrated at $E \simeq 20$ MeV must take place not only through the neutron disintegration channels but also, with less probability, through the proton channels, and this corresponds to the results of Refs. 55 and 56.

The decays of the dipole excitations of ^{13}C to the states of the daughter nuclei with $T_f = 1$ take place primarily with population of the levels $1^+ T = 1$ ($E = 15.11$ MeV) and $2^+ T = 1$ ($E = 16.11$ MeV) of the ^{12}C nucleus and their isobar analogs (with $E = 0$ and $E = 0.95$ MeV) in the ^{12}B nucleus. Calculations, both in a complete $1\hbar\omega$ basis[29] (Fig. 17) and in the PFNS approach,[38] reproduce the gross structure of the partial cross sections of these channels at least at the level of the 20% accuracy of the measurements.[59]

Photodisintegration of ^{15}N

Measurements have been made of the partial photoneutron cross sections for ^{15}N disintegration to not only the ground state[68] but also the excited states[70] of ^{14}N. In the photoproton channel, transitions to the ground state,[75,92] and excited states[70,75] of ^{14}C have also been identified. Transition to the ^{14}C ground state has also been observed[93] in the ^{15}N electrodisintegration reaction. There have been a number of studies of the inverse reactions: $^{14}C(p, \gamma_0)^{15}N$ (Ref. 94), $^{14}N(p, \gamma_0)^{15}O$ (Refs. 52 and 95), and $^{14}N(n, \gamma_0)^{15}N$.[96] There are experimental data on the deuteron[93] and triton[70] disintegration channels for ^{15}N.

The partial integrated cross section through the channel $^{15}N(\gamma, ^3H)^{12}C$ (4.4 MeV) was found[70] to be 7 MeV · mb in the interval of excitation energies up to $E^* = 35$ MeV, and through the $^{15}N(\gamma, d)^{13}C_{g.s}$ channel to be 1.0 ± 0.3 MeV · mb up to $E^* = 25$ MeV.

A series of studies has been made of inverse photonuclear reactions induced by light ions: $^{13}C(d, \gamma)^{15}N$ (Refs. 96 and 97), $^{12}C(^3H, \gamma)^{15}N$ (Ref. 98), $^{12}C(^3He, \gamma)^{15}N$ (Ref. 99), and $^{11}B(\alpha\gamma)^{15}N$.[100]

The levels of the ^{14}N and ^{14}C nuclei most strongly populated by photodisintegration of ^{15}N through the nucleon channel are given in Table IX. The pronounced discrepancy between the results of the two measurements of the cross section in the $(\gamma, p_{7.01})$ channel stands out. It should be noted that although the method employed in Ref. 75 made it possible to find the cross section associated with the $(\gamma, p_{8.32})$ channel, this was not done. It is quite possible that this cross section was added to the $(\gamma, p_{7.01})$ cross section. But even then the discrepancy between the two measurements is not eliminated.

The $J^\pi T = 2^+ 1$ levels with energies $E^* = 7.01$ MeV and $E^* = 8.32$ MeV of the ^{14}C nucleus are interesting in that the shell configuration $|s^4p^{10}\,{}^3{}^1D_2\rangle$ ($|p_{3/2}^{-1}p_{1/2}^{-1}\rangle$ in the jj-coupling representation) has been divided almost equally between them, as indicated, in particular, by the spectroscopic factors (see Table IX). The same situation is found in ^{14}N for the levels with the same quantum numbers ($E^* = 9.17$ MeV and $E^* = 10.43$ MeV). In ^{14}N, both levels lie above the threshold of subsequent decay through the pro-

ton channel, while in ^{14}C one of them is bound, the other being just above (by 150 keV) the neutron threshold.

According to the calculations of Refs. 33 and 34, the $T_<$ branch of the resonance in ^{15}N decays predominantly (in approximately 70% of the cases) to levels of the ^{14}N nucleus with isospin $T_f = 0$. The remaining 30% is to levels of the nucleus ^{14}C (proton channel) and ^{14}N with isospin $T_f = 1$ in a ratio $\approx$4:1. The geometrical factor leads to the ratio 2:1. But since the proton threshold is below the neutron threshold, and the orbital angular momentum of the majority of the emitted nucleons is $1 = 2$, the ratio deviates from the geometrical value. According to the calculations of Refs. 33 and 34, about 10% of the integrated cross section of the $T_<$ branch and not more than 15% of the complete resonance is associated with transitions to the negative-parity levels of the ^{14}C nucleus due to the shake-off effect. The experimental data of Ref. 70 also indicate weak population of such states.

The partial cross sections to the levels with $T_f = 0$ of the ^{14}N nucleus are given in Fig. 18 together with the calculated cross section of total absorption in the $T_<$ branch. It follows from the calculation that more than half of the integrated cross section of the $T_<$ branch is concentrated in the region of excitations of the ^{15}N nucleus from 21 to 25 MeV. However, in the (γ, n_0) channel the high-energy part of the spectrum is very empty and does not correspond to the observed picture. The situation found in ^{13}C is repeated.

The high-energy region of excitation of the nucleus with isospin $T_<$ has a stronger fractional-parentage coupling to the excited states of ^{14}N. The experimental data also indicate such an effect. However the accuracy of the measurements, which is not better than 30%, does not permit more definite conclusions. The three levels considered take half of the total-absorption cross section corresponding to the $T_<$ branch (theory of Refs. 33 and 34). Therefore, the transitions to them reflect to a considerable degree the structure of the $T_<$ branch of the resonance in ^{15}N. In this connection, it is important to make new measurements of the transitions to the excited states of ^{14}N with $T_f = 0$ with higher accuracy, since this will help to establish the high-energy part of the $T_<$ branch of the dipole resonance.

We now consider the population of the levels with $T_f = 1$ in ^{14}N and of the levels of the ^{14}C nucleus. The partial cross sections in the (γ, p) channel to three levels of the ^{14}C nucleus (ground state, $J^\pi T = 2^+ 1, E^* = 7.01$ MeV, and $J^\pi T = 1^+ 1 E^* = 10.7$ MeV) are given in Fig. 19. Figure 19a gives the cross section of the photoproton reaction converted[95] from the experimental data on the inverse (p, γ_0) reaction.

The maximum in the cross section of the (γ, p_0) reaction was found to be at excitation energy $E^* = 24.4$ MeV and due to the decay of the state that forms the main maximum in the total-absorption cross section.

Figure 19c gives the partial cross section to the level $J^\pi T = 2^+1, E^* = 7.01$ MeV in the ^{14}C nucleus. The experimental data are contradictory. It follows from the calculation of Refs. 33 and 34 that the maximum in the $(\gamma, p_{7.01})$ cross section is associated with the decay of the state that forms the main maximum in the total-absorption cross section and the decay of a state $J^\pi T = 1/2^+ 3/2$ situated at a slightly lower energy.

Figure 19d gives the partial cross section[75] to the level $J^\pi T = 1^+ 1, E = 10.7$ MeV and the result of the calculation of Refs. 33 and 34. The theory again attributes the maximum to the decay of the state that forms the main maximum in the

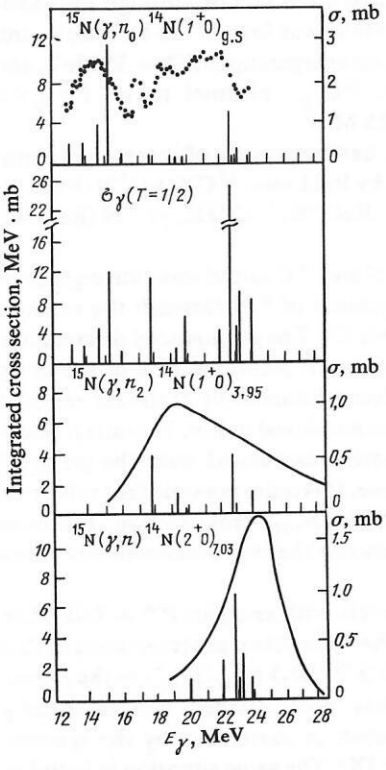

FIG. 18. Partial cross sections of ^{15}N photodisintegration into levels of the ^{14}N nucleus with $T_f = 0$: theory (vertical lines) of Refs. 33 and 34 and experiment (points) of Refs. 68 and 70; the continuous curves are from Ref. 70.

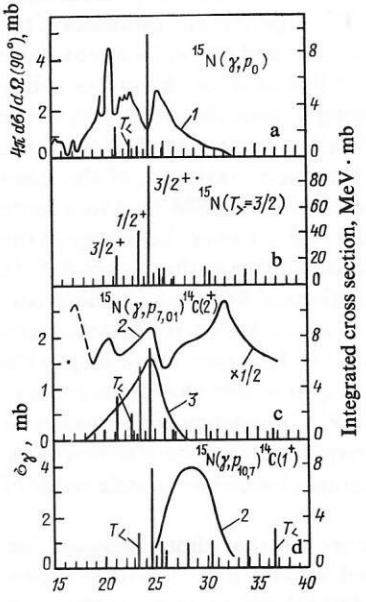

FIG. 19. partial cross sections of ^{15}N photodisintegration to levels of the nuclei ^{14}C and ^{14}N with $T_f = 1$: 1) Ref. 95; 2) Ref. 75; 3) Ref. 70.

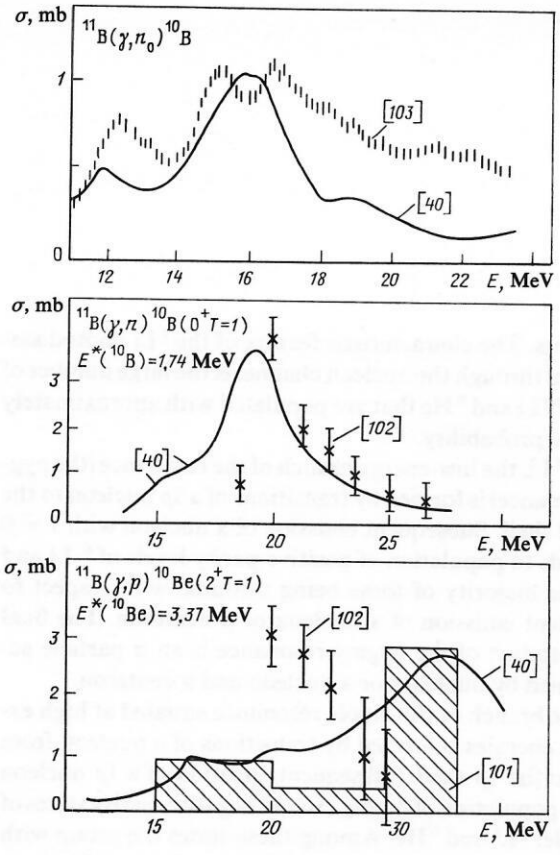

FIG. 20. Partial cross sections of ^{11}B photodisintegration: theory of Ref. 40 (continuous curves) and experiment of Refs. 101–103 (references are indicated in square brackets).

total-absorption cross section. The observed maximum is 4 MeV higher.

The nucleus ^{11}B

Data on the partial cross sections of ^{11}B photodisintegration from the experiments of Ref. 101 and 102 and the results of a calculation using the PFNS basis[40] are given in Fig. 20. Table XVIII gives the distribution of the total photodisintegration cross section over intervals of excitation energies as obtained in this calculation for different spins and isospins of the ^{11}B dipole excitation. Table XIX gives the levels of the daughter nuclei ^{10}B and ^{10}Be that are most strongly populated by the photodisintegration of ^{11}B. The "friability" of the ground-state structure of this nucleus is manifested in the broad spectrum of hole states and a correspondingly large number of partial photodisintegration channels.

Transitions to the $T=0$ states of the ^{10}B nucleus are associated with decay of the $T=1/2$ branch of the dipole resonance, this branch in the case of the ^{11}B nucleus being distributed over the complete interval of dipole excitation energies (Fig. 9). According to Ref. 40, the decay of the $T=1/2$ branch of the giant dipole resonance in the region of energies above 20 MeV takes place predominantly to excited $T=0$ states of ^{10}B. Comparison of the $\sigma(\gamma, n_0)$ data of Ref. 103 with the results of the calculation (Fig. 20) shows that the theory underestimates the mixing of the dipole excitations coupled to the various hole states, and as a result of this gives an underestimate of the cross section $\sigma(\gamma, n_0)$ of the reaction in the region $E>19$ MeV. The data on population of the 2^+ $T=0$ state of ^{10}B ($E=3.59$ MeV) obtained in $(\gamma, p\gamma')$ and $(\gamma, n\gamma')$ experiments[101,102] are contradictory and need to be made more accurate. The result of calculation in the PFNS approach corresponds to the distribution of Ref. 101—the partial cross section is distributed over a wide energy interval from 15 to 30 MeV, has no sharp peaks and passes through a minimum at $E=$ 20–25 MeV.

Decays to the $T=1$ levels of the final nuclei take place mainly from the $T=3/2$ branch, although the contribution of the $T=1/2$ branch is important at $E=$ 15–17 MeV. For transitions to the 0^+ $T=1$ state, the calculation reproduces well the data of the ^{11}B$(\gamma, n_{1.74})$ ^{10}B reaction[102] (Fig. 20). The same curve corresponds to the behavior of the (γ, p_0) partial cross section. Almost the entire intensity of the decay to this level is associated with the excitation $5/2^+$ $T=3/2$ ($E=19.2$ MeV).

According to the experimental data of Ref. 101 and the calculation of Ref. 40, the transitions to the 2^+ $T=1$ state of the ^{10}Be nucleus ($E=3.37$ MeV) have a maximum at $E=$ 25–28 MeV. In contrast, the experiment of Ref. 102 indicates a peak in this partial cross section at $E=20$ MeV. The contradictory nature of these data is due to the complexities of obtaining information on the partial cross sections in the cases when the levels of the daughter nuclei are separated by small energy intervals and indicates the need for more accurate experiments.

TABLE XVIII. Distribution of photoabsorption cross section over dipole excitation states of ^{11}B, MeV · mb (Ref. 40).

E_1-E_2, MeV	$J_f=1/2$		3/2		5/2		Σ
	$T_f=1/2$	3/2	1/2	3/2	1/2	3/2	
$E<14.5$	0.1	1.67	3.0	0	4.28	0	9.05
14.5–17.5	2.5	0	1.32	0	3.57	0	7.39
17.5–21.0	0.92	0.25	1.33	3.04	0.10	9.55	15.18
21.0–30.0	0.11	5.35	7.96	25.58	4.10	27.78	70.88
$E>30$	5.38	0.98	6.83	3.72	23.65	14.84	55.40
Σ	9.01	8.25	20.43	32.34	35.70	52.17	157.9

TABLE XIX. Distribution of partial decay cross sections of dipole excitations of the nucleus ^{11}B (excitation energy $E < 30$ MeV), MeV · mb (Ref. 40).

Final nucleus	J^π	T	E, MeV	Σ_i	Final nucleus	J^π	T	E, MeV	Σ_i
^{10}B	3+	0	0	10		3+	0	4.77	1
	1+	0	0.72	6		0+	1	1.74	9
	1+	0	2.15	6		2+	1	5.17	21
	2+	0	3.59	4	^{10}Be	0+	1	0	9
	2+	0	5.92	1		2+	1	3.37	20

The nucleus ^{14}C

The absorption of photons by the ^{14}C nucleus leads to dipole excitations with isospin $T = 1$ and $T = 2$ (see Fig. 2). The ground state of the ^{14}C nucleus is the isobar analog of the excited 0^+ $T = 1$, $E = 2.31$ MeV state of the ^{14}N nucleus. The main branches of photoexcitation with $T = 2$ for these two states are identical. The difference between the photoexcitation functions is due solely to the branches $T_<$: $T = 1$ for the ^{14}C nucleus and $T = 0$ for the excited ($E = 2.31$ MeV) level of the ^{14}N nucleus.

The ratio of the excitation cross sections for the isospin branches is close to the ratio of the corresponding geometrical factors. It is important that the structure of these resonance curves is not similar to the structure of the curve of the photoexcitation above the ground state of the ^{14}N nucleus, and the displacement of the maxima of the curves is not equal to the excitation energy of a basis state.

The probability of decay of the dipole resonance in the ^{14}C nucleus through the (γ, n) and $(\gamma, 2n)$ channels exceeds by almost two orders of magnitude the probability of decay with emission of charged particles. The results of the calculation of Ref. 31 of the distribution of the photodisintegration over the channels are given in Table XX. The strongly collectivized principal maximum of the giant dipole resonance ($E \approx 26$ MeV) decays predominantly to the level of the ^{13}C nucleus with $3/2^- T = 3/2$, $E = 15.1$ MeV, which then decays further through the neutron (γ, n_1) channel $(^{13}\mathrm{C})^* \to n + {}^{12}\mathrm{C}_{4.43}$ or, with lesser widths, through the (γ, n_0) channel and channels with photon emission.

6. PHOTODISINTEGRATION OF THE NUCLEI ^{7}Li AND ^{9}Be

The results of the calculation in Ref. 20 of the partial cross sections of ^{7}Li photodisintegration through the nucleon channel in the variant COP BSM($1\hbar\omega$) are given in Table XXI. Also given there are the results of various measurements. The characteristic feature of the ^{7}Li photodisintegration through the nucleon channel is the large number of levels of ^{6}Li and ^{6}He that are populated with approximately the same probability.

In ^{7}Li, the low-energy branch of the resonance (the pygmy resonance) is formed by transitions of a $1p$ nucleon to the $2s$ or $1d$ shell. Subsequent emission of a nucleon with $1 = 0$ or 2 leads to population of positive-parity levels of ^{6}Li and ^{6}He, the majority of these being unstable with respect to subsequent emission of a nucleon or a deuteron. The final decay product of the pygmy resonance is an α particle accompanied by nucleons or a nucleon and a deuteron.

The branch of the dipole resonance situated at high excitation energies is formed by transitions of a nucleon from the $1s$ to the $1p$ shell. Subsequent emission of a $1p$ nucleon leads to population of highly excited negative-parity states of the nuclei ^{6}Li and ^{6}He. Among these states the group with energy around 20 MeV, with which about 25% of the total-absorption cross section is associated, is interesting. The structure of the wave function of this group of levels is such that one must expect strong decay of ^{6}Li to $^3\mathrm{He} + {}^6\mathrm{H}$ and of ^{3}He to $^3\mathrm{H} + {}^3\mathrm{H}$. Thus, the high energy branch of the resonance in ^{7}Li undergoes a star decay but among the products there are no α particles.

The predominantly star nature of the ^{7}Li disintegration makes it necessary to set up coincidence experiments. So far, a number of such measurements have been made.[107] Coincidence of only two particles was recorded. However, more detailed quantitative information is needed on the energy and angular characteristics. From the theoretical point of view, an important part could be played by calculations in the framework of the Faddeev equations with forbidden states,[108,109] which make it possible to take into account the interaction of the particles in the final states in the channels $\gamma + {}^7\mathrm{Li} \to {}^3\mathrm{H} + {}^3\mathrm{H} + p$ and $\gamma + {}^7\mathrm{Li} \to {}^3\mathrm{He} + {}^3\mathrm{H} + n$.

The supermultiplet structure of the ^{9}Be and ^{8}Be levels

TABLE XX. Distribution of probabilities of photodisintegration of the ^{14}C nucleus[31] over the states of the final nuclei.

Final nucleus $J^\pi T$	^{13}C					^{12}C		
	1/2− 1/2	3/2− 1/2	5/2− 1/2	7/2− 1/2	3/2− 3/2	0+0	2+0	
E, MeV	0	3.68	7.55	10.75	15.11	0	4.44	Unstable levels
Fraction of integrated cross section, %	11.3	12.6	7.0	4.8	37	4.3	17.0	6.6

TABLE XXI. Photodisintegration of ^{7}Li through the nucleon channel in the BSM ($1\hbar\omega$) approach in the COP variant[20] (references are given in square brackets).

Channel (γ, n)					Channel (γ, p)			
Final state		Partial cross section		Subsequent decay	Final state, E^*, MeV	Partial cross section		Subsequent decay
$J\pi T$	E^*, MeV	MeV · mb	%			MeV·mb	%	
1+0	0	5.8	5	—	—	—	—	—
3+0	2.18	7.9	7	—	—	—	—	—
		2.0 [86]	—	$\alpha+d$	—	—	—	—
0+1	3.56	6.4	6	—	0	4.3	4	β
		5.0 [86]	—	γ	—	14.4±6 [105]		—
		11±3 [104]	—	—	—	15 [106]		—
2+0	4.31	5.8	5	—	—	—	—	—
2+1	5.37	9.6	8	$\alpha+d$	1.80	8.2	7	$\alpha+2n$
1+0	5.65	0.7	1	γ	—	—		—
Remaining positive-parity levels (10–17 MeV)		9	8	$\alpha+np$		2	2	$\alpha+2n$
Sum over all positive-parity levels		45	39	—	—	14	12	—
2−1	19.9	18	16	^{3}He+^{3}H	17.9	7	6	^{3}H+^{3}H
1−1	20.8	5	4		18.8	1	1	
Remaining negative-parity levels		19	17	—	—	5	4	—
Sum over all negative-parity levels		42	37	—	—	13	11	—
Sum over all levels		87	76	—	—	27	24	—

strongly influences the decay of the photonuclear resonance in ^{9}Be. The dominant component of the ground-state wave function of ^{9}Be is $1s^4\,1p^5$ [441] (see Table II). The doorway states forming the skeleton of the dipole resonance are states with Young diagrams [441]$T = 1/2$, [432]$T = 1/2$ and 3/2, [4311]$T = 1/2$ and 3/2. The decay of the dipole resonance to the ground and excited states up to excitation energy 16 MeV (the Young diagram of the wave function of these states has the form [44]) of the ^{8}Be nucleus can take place only by virtue of configurations with the Young diagram [441]. However, the importance of these configurations in forming the dipole resonance is slight.[110] Therefore, the first three levels of ^{8}Be are weakly populated.

The decay of the dipole resonance in ^{9}Be is associated primarily with population of highly excited states (beginning with 16.6 MeV) of the ^{8}Be nucleus. The subsequent decay leads to emission of nucleons, deuterons, or α particles. These channels were considered in detail in Refs. 110–112 (see also Ref. 6).

CONCLUSIONS

We have considered in detail the energy dependence of the total photoabsorption cross sections and the partial photonucleon cross sections from the point of view of both theory and the experimental material. The modern models using a large basis to construct the wave functions of the states of the giant dipole resonance basically give a good qualitative description of the existing experimental data on the total absorption. All models give practically the same gross structure of the total-absorption spectrum. The experimental data do not permit a choice to be made between the computational variants. However, in all cases the theory overestimates the concentration of the dipole-resonance strengths. This fact calls for further efforts aimed at the inclusion of a new source of spreading. Such could be $2\hbar\omega$ excitations. To implement such a program in the $1p$-shell nuclei systematically, it would appear to us to be more expedient to start from the PFNS variant of the theory and include the higher

excitations by using, for example, the strength-function technique proposed in Ref. 113.

As follows from the analysis made here, study of the partial cross sections has made possible a further important step in the study and understanding of the nature of the dipole resonance. In numerous cases the theory reproduces the main features obtained experimentally. Naturally, at the deeper level there have arisen a number of problems that are not yet understood and explained. In the first place, this is due to the manner in which the ground state is populated, the pygmy resonance decays, and some other factors. Of course, the present state of the theory does not yet make it possible to encompass at the microscopic level many important aspects in the description of the decay properties of the resonance, in particular, the part played by pre-equilibrium and equilibrium processes. At this level too it also appears important to investigate fully the part played by the $2\hbar\omega$ excitations.

It should be noted that in many cases the results of measurements made in different laboratories strongly contradict one another. It is important to make more systematic investigations of the partial cross sections.

Recently, data on the angular distributions of nucleons in partial transitions have become available. This question has not been treated in the present review. In the shell model in the BSM variant this characteristic has hardly been analyzed. Of course, the possibilities of the BSM are here limited—the interference effects that complicate the picture cannot be taken into account. Nevertheless, it would seem to be important to consider such a characteristic even with these limitations.

Of course, the theory based on the CSM takes into account these effects. But in it the problem of the spreading of the resonance becomes acute. One of the steps by which such spreading can be taken into account is associated with the use of an optical potential. However, as analysis of the partial spectra shows, it is necessary to include a number of strong states directly.

Concluding the review, we note that an important step in describing the decay properties of the dipole resonance has been made. But at the same time this step has raised a number of new problems. Subsequent investigations must find the answers to them.

[1]V. G. Neudachin, V. G. Shevchenko, and N. P. Yudin, in: *Yadernye reaktsii pri malykh i srednikh énergiyakh* (*Nuclear Reactions at Low and Intermediate Energies*), Nauka, Moscow (1962), p. 486; Phys. Lett. **10**, 180 (1964).
[2]V. G. Neudachin and V. N. Orlin, Nucl. Phys. **31**, 338 (1962).
[3]R. A. Éramzhyan, Izv. Akad. Nauk SSSR, Ser. Fiz. **28**, 1181 (1964).
[4]V. G. Shevchenko, in: *Tr. Mezhdunarodnoĭ konferentsii po élektromagnitnym vzaimodeĭstviyam pri nizkikh i srednikh énergiyakh* (*Proc. of the Intern. Conf. on Electromagnetic Interactions at Low and Intermediate Energies*), Vol. 3, Nauka, Moscow (1967), p. 206.
[5]V. G. Neudachin, *ibid.*, p. 351.
[6]B. S. Ishkhanov *et al.*, Fiz. Elem. Chastits At. Yadra **12**, 905 (1981); **14**, 286 (1983) [Sov. J. Part. Nucl. **12**, 362 (1981); **14**, 119 (1983)].
[7]L. S. Cardman, Nucl. Phys. **A354**, 173 (1981).
[8]S. S. Hanna, Lect. Notes Phys. **108**, 288 (1977).
[9]J. M. Dixon, *Proc. of the Intern. Conf. on Photonuclear Reactions and Applications*, Asilomar (1973), p. 727.
[10]R. Bergere, Lect. Notes Phys. **61**, 1 (1977).
[11]Kh. U. Eger, H.-R. Kissener, and R. A. Éramzhyan, in: *Élektromagnitnye vzaimodeĭstviya yader pri malykh i srednikh énergiyakh* (*Electromagnetic Interactions of Nuclei at Low and Intermediate Energies*), Nauka, Moscow (1973), p. 63.
[12]V. V. Balashov *et al.*, Nucl. Phys. **A129**, 369 (1969).
[13]C. Mahaux and H. A. Weidenmüller, *Shell-Model Approach to Nuclear Reactions*, North-Holland Amsterdam (1969).
[14]I. Rotter *et al.*, Fiz. Elem. Chastits At. Yadra **6**, 435 (1975) [Sov. J. Part. Nucl. **6**, 175 (1975)].
[15]J. Höhn, H. W. Barz, and I. Rotter, Nucl. Phys. **A330**, 109 (1979).
[16]A. M. Lane and R. G. Thomas, Rev. Mod. Phys. **30**, 257 (1958) [Russian translation published by Izd. Inostr. Lit., Moscow (1960)].
[17]M. Marangoni, P. L. Ottaviani, and A. M. Saruis, Nucl. Phys. **A277**, 239 (1977).
[18]S. Cohen and D. Kurath, Nucl. Phys. **73**, 1 (1965); **101**, 1 (1967).
[19]A. N. Boyarkina, *Struktura yader p-obolochki* (*Structure of p-Shell Nuclei*), Moscow State University (1973).
[20]H. R. Kissener, *Dr. Sc. Thesis, Techn. Univ.*, Dresden (1981).
[21]R. A. Sakaev and R. A. Éramzhyan, *Soobshcheniya* (*Communication*), R2-9610, JINR, Dubna (1976).
[22]J. D. Vergados, Nucl. Phys. **A239**, 271 (1975).
[23]B. S. Cooper and J. M. Eisenberg, Nucl. Phys. **A14**, 184 (1968).
[24]A. Aswad, H. R. Kissener *et al.*, Nucl. Phys. **A208**, 61 (1973).
[25]H. R. Kissener and R. A. Éramzhyan, in: *Proc. of the Intern. Conf. on Nuclear Physics with Electromagnetic Interactions*, Vol. 2, Mainz (1979), p. 20.
[26]W. D. Teeters and D. Kurath, Nucl. Phys. **A283**, 1 (1977).
[27]D. J. Rowe and S. S. M. Wong, Nucl. Phys. **A153**, 561 (1970).
[28]N. Ohtsuka, Ph.D thesis, Osaka University (1978).
[29]H. R. Kissener, A. Aswad *et al.*, Nucl. Phys. **A219**, 601 (1974).
[30]H. U. Jäger, H. R. Kissener, and R. A. Éramzhyan, Nucl. Phys. **A171**, 16, 584 (1971).
[31]H. R. Kissener, R. A. Éramzhyan, and H. U. Jäger, Nucl. Phys. **A207**, 78 (1973).
[32]H. R. Kissener and R. A. Éramzhyan, Nucl. Phys. **A326**, 289 (1979).
[33]M. A. Zhusupov and R. A. Éramzhyan, Izv. Akad. Nauk SSSR, Ser. Fiz. **33**, 730 (1969).
[34]V. V. Karapetyan, M. A. Zhusupov, and R. A. Éramzhyan, *Soobshcheniya* (*Communication*) R4-3177, JINR, Dubna (1967).
[35]N. G. Goncharova and N. P. Yudin, Yad. Fiz. **12**, 725 (1970) [Sov. J. Nucl. Phys. **12**, 392 (1971)]; Phys. Lett. **B29**, 272 (1969).
[36]J. Birkholz, Nucl. Phys. **A189**, 385 (1972).
[37]N. G. Goncharova, Czech. J. Phys. **B32**, 225 (1982).
[38]N. G. Goncharova and G. S. Sagiyan, Vestn. Mosk. Univ. **13**, 118 (1972).
[39]N. G. Goncharova, Yad. Fiz. **15**, 242 (1972) [Sov. J. Nucl. Phys. **15**, 137 (1972)].
[40]N. G. Goncharova, B. S. Ishkhanov, and V. I. Mokeev, Yad. Fiz. **35**, 43 (1982) [Sov. J. Nucl. Phys. **35**, 26 (1982)].
[41]A. N. Gol'tsov and N. G. Goncharova, Yad. Fiz. **38**, 1410 (1983) [Sov. J. Nucl. Phys. **38**, 857 (1983)].
[42]V. Gillet and N. Vinh-Mau, Nucl. Phys. **54**, 321 (1964).
[43]V. Gillet and E. A. Sanderson, Nucl. Phys. **54**, 472 (1964).
[44]D. J. Millener and D. Kurath, Nucl. Phys. **A255**, 315 (1975).
[45]H. U. Jäger and M. Kirchbach, Nucl. Phys. **A291**, 52 (1977).
[46]J. Ahrens *et al.*, Nucl. Phys. **A251**, 479 (1975).
[47]N. Bezić *et al.*, Nucl. Phys. **A128**, 426 (1969).
[48]A. S. Cherkasov, Yad. Fiz. **28**, 639 (1978) [Sov. J. Nucl. Phys. **28**, 328 (1978)]; Yu. M. Arkatov *et al.*, Yad. Fiz. **19**, 1172 (1974) [Sov. J. Nucl. Phys. **19**, 598 (1974)].
[49]A. M. Saruis and M. Marangoni, Nucl. Phys. **A132**, 433, 649 (1969).
[50]M. Kirchbach and H. R. Kissener, ZfK K-336, Rossendorf (1977), p. 111.
[51]J. S. Dehesa, Ph.D. thesis, Rheinischen F. W. Universität zu Bonn (1978).
[52]H. R. Weller *et al.*, Phys. Rev. C **13**, 922 (1976).
[53]R. J. Hughes *et al.*, Nucl. Phys. **A215**, 147 (1973); **A238**, 189 (1975).
[54]U. Kneissl *et al.*, Nucl. Phys. **A264**, 30 (1976).
[55]J. W. Jury, B. L. Berman *et al.*, Phys. Rev. C **19**, 1684 (1979).
[56]D. Zubanov *et al.*, Phys. Rev. C **27**, 1957 (1983).
[57]D. J. Albert *et al.*, Phys. Rev. C **16**, 503 (1977).
[58]B R. Easlea, Phys. Lett. **1**, 163 (1962).
[59]B. H. Patrick *et al.*, J. Phys. G **1**, 874 (1975).
[60]J. W. Jury *et al.*, Phys. Rev. C **26**, 777 (1982).
[61]H. Arenhövel, Lect. Notes Phys. **108**, 159 (1979).
[62]N. A. Burkova and M. A. Zhusupov, *Fizika vysokikh énergiĭ i variatsii kosmicheskikh lucheĭ* (*High Energy Physics and Variations in Cosmic Rays*), Alma-Ata (1982), p. 50.
[63]J. Källne and E. Hagberg, Phys. Scr. **4**, 151 (1971).

[64]I. S. Towner, Nucl. Phys. **A126**, 97 (1969).
[65]J. L. Snelgrove *et al.*, Phys. Rev. **187**, 1259 (1969).
[66]H. Taketani *et al.*, Phys. Lett. **B27**, 625 (1968).
[67]L. J. Parish *et al.*, Phys. Rev. C **9**, 876 (1974).
[68]J. D. Watson *et al.*, Phys. Rev. C **27**, 506 (1983).
[69]R. Kosiek *et al.*, Phys. Lett. **9**, 260 (1969); Z. Phys. **174**, 337 (1963).
[70]B. H. Patrick *et al.*, J. Phys. G **2**, 751 (1976).
[71]J. W. Jury *et al.*, Nucl. Phys. **A337**, 503 (1980).
[72]J. E. E. Baglin *et al.*, Phys. Rev. C **10**, 24 (1974).
[73]D. Berghofer *et al.*, Nucl. Phys. **A263**, 109 (1976).
[74]J. G. Woodworth *et al.*, Can. J. Phys. **55**, 1704 (1977).
[75]V. P. Denisov *et al.*, Yad. Fiz. **14**, 889 (1971) [Sov. J. Nucl. Phys. **14**, 497 (1972)].
[76]H. A. Medicus *et al.*, Nucl. Phys. **A156**, 257 (1970).
[77]B. S. Ishkhanov *et al.*, Yad. Fiz. **32**, 305 (1980) [Sov. J. Nucl. Phys. **32**, 157 (1980)].
[78]R. G. Allas *et al.*, Nucl. Phys. **58**, 122 (1964).
[79]M. T. Collins, Phys. Rev. C **26**, 332 (1982).
[80]S. S. Hanna, Nucl. Phys. **A358**, 229 (1981).
[81]E. D. Mshelia and R. F. Barrett, Z. Phys. **261**, 313 (1973).
[82]R. W. Gellie *et al.*, Can. J. Phys. **50**, 1689 (1972).
[83]P. Paul *et al.*, Nucl. Phys. **A254**, 1 (1975).
[84]N. N. Thompson *et al.*, Phys. Lett. B **31**, 211 (1970).
[85]N. K. Sherman *et al.*, Phys. Rev. Lett. **25**, 114 (1970).
[86]B. S. Ishkhanov *et al.*, Yad. Fiz. **32**, 11 (1980) [Sov. J. Nucl. Phys. **32**, 5 (1980)].
[87]R. M. Carr *et al.*, Phys. Rev. C **6**, 2032 (1972).
[88]A. P. Komar *et al.*, Nucl. Phys. **34**, 551 (1962).
[89]A. N. Gorbunov *et al.*, Zh. Eksp. Teor. Fiz. **42**, 551 (1962) [Sov. Phys. JETP **15**, 386 (1962)].
[90]P. Van Otten *et al.*, Annual Report of Ghent Univ. (1982), p. 38.
[91]G. A. Fisher, Ph.D. thesis, Stanford Univ. (1970).
[92]R. Kosiek, Z. Phys. **179**, 544 (1964).
[93]J. J. Murphy *et al.*, Nucl. Phys. **A246**, 221 (1975).
[94]W. J. O'Connell *et al.*, Bull. Am. Phys. Soc. **14**, 508 (1969).
[95]M. H. Harakeh *et al.*, Phys. Rev. C **12**, 1410 (1975).
[96]W. Del Bianco *et al.*, Nucl. Phys. **A270**, 45 (1976); Can. J. Phys. **56**, 3 (1978).
[97]H. R. Weller *et al.*, Nucl. Phys. **A211**, 221 (1973).
[98]M. Schaeffer *et al.*, Nucl. Phys. **A275**, 1 (1977).
[99]W. Del Bianco *et al.*, Can. J. Phys. **56**, 1054 (1978).
[100]A. Degre *et al.*, Nucl. Phys. **A306**, 77 (1978).
[101]B. H. Patrick *et al.*, Phys. Lett. **B34**, 488 (1971).
[102]A. S. Alimov *et al.*, Yad. Fiz. **40**, 301 (1984) [Sov. J. Nucl. Phys. **40**, 190 (1984)].
[103]H. M. Kuan *et al.*, Nucl. Phys. **A151**, 129 (1970).
[104]V. P. Denisov, Yad. Fiz. **27**, 882 (1978) [Sov. J. Nucl. Phys. **27**, 469 (1978)].
[105]V. P. Denisov and I. Ya. Chubukov, Yad. Fiz. **20**, 1106 (1974) [Sov. J. Nucl. Phys. **20**, 579 (1975)].
[106]A. G. Gregory *et al.*, Nucl. Phys. **32**, 543 (1962).
[107]G. Junghans *et al.*, Z. Phys. A **291**, 353 (1979).
[108]B. I. Kukulin *et al.*, Yad. Fiz. **24**, 298 (1976) [Sov. J. Nucl. Phys. **24**, 155 (1976)]; J. Phys. G **4**, 1409 (1978).
[109]V. I. Kukulin, V. G. Neudachin, and Yu. F. Smirnov, Fiz. Elem. Chastits At. Yadra **10**, 1236 (1979) [Sov. J. Part. Nucl. **10**, 492 (1979)].
[110]L. Majling *et al.*, Czech. J. Phys. **B18**, 1560 (1968); Phys. Lett. **27**, 487 (1968).
[111]A. Buchnea *et al.*, Can. J. Phys. **56**, 47 (1976).
[112]V. P. Denisov and L. A. Kul'chitskiĭ, Yad. Fiz. **3**, 268 (1966); **5**, 490 (1967) [Sov. J. Nucl. Phys. **3**, 192 (1966); **5**, 344 (1967)].
[113]L. A. Malov and V. G. Solov'ev, Fiz. Elem. Chastits At. Yadra **11**, 301 (1980) [Sov. J. Part. Nucl. **11**, 111 (1980)].
[114]J. H. Wyckoff *et al.*, Phys. Rev. **137**, B576 (1965).
[115]H. Ferdinande *et al.*, Can. J. Phys. **55**, 428 (1977).
[116]E. Kerkhove *et al.*, Phys. Rev. C **29**, 2061 (1984).

Translated by Julian B. Barbour